This is to certify that the

dissertation entitled

DIRECT GENERATION OF EFFICIENT LOW-ORDER MODELS FOR LINEAR MIXED-STRUCTURE SYSTEMS

presented by

William Frederick Resh

has been accepted towards fulfillment
of the requirements for

Ph.D. degree in **Mechanical Engineering**

R. C. Lamberg
Major professor

Date July 27, 1984

DIRECT GENERATION OF EFFICIENT LOW-ORDER MODELS FOR LINEAR MIXED-STRUCTURE SYSTEMS

By

William Frederick Resh

A DISSERTATION

Submitted to
Michigan State University
in partial fulfillment of the requirements
for the degree of

DOCTOR OF PHILOSOPHY

Department of Mechanical Engineering

1984

ABSTRACT

DIRECT GENERATION OF EFFICIENT LOW-ORDER
MODELS FOR LINEAR MIXED-STRUCTURE SYSTEMS

By

William Frederick Resh

Many physical systems consist of lumped-parameter subsystems coupled by continuum elements. For example, in an automotive drivetrain the engine, transmission, differential, and wheels could be represented as lumped-parameter systems and the drive shaft and axles as continuum elements. In modelling these mixed-structure systems, the continuum elements give rise to partial differential equations and the discrete subsystems give rise to ordinary differential equations. Because of the coupling between the subsystems, analytical solutions are unobtainable in general.

Typical modelling approaches for these problems discretize the continuum elements, using large numbers of local variables in order to get an accurate representation of the entire system's behavior. Often, because of the model's size, it is very expensive to work with directly, particularly in an iterative design context. One way to try to achieve efficiency in the design process for linear systems is to apply a model-order reduction procedure to the large-order model to

obtain a lower-order working model. In this work, a procedure is developed that permits forming an efficient low-order model directly, bypassing the formulation of the large-order model and application of a model-order reduction procedure. A procedure of this type is especially attractive for use in preliminary design, where constraints on time and computational resources may prohibit iterative analyses of large systems models.

The particular type of linear mixed-structure systems to be examined are those having a cascade structure. A procedure is developed based on parameter information, coupling effects, and tabulated error results for some prototype cases. Applications of the procedure are illustrated.

ACKNOWLEDGEMENTS

I would like to thank Ronald Rosenberg for the many timely and insightful discussions we had, my wife for her support and patience, and my parents for their support and interest through the years.

TABLE OF CONTENTS

LIST OF TABLES

LIST OF FIGURES

1. INTRODUCTION

1.1 Background

Many dynamical problems of practical interest are linear mixed-structure systems. That is, they consist of linear subsystems that are inherently discrete coupled by linear continuum elements. See Figure 1.1 for an abstract representation. The continua are shown with each one coupling two discrete subsystems, which is the most common case in engineering systems. Consider, for example, the rotational positioning mechanism shown in Figure 1.2. In the process of modelling the dynamics of such a system, the engineer is faced with the problem of using finite dimensional models of the two shafts. Two questions emerge in this problem. The first of these is: How should one discretize each shaft in order to get a reasonable model of it? Contained in this question is the matter of the type of discretization to use (eg., finite elements) and the number of elements or degrees-of-freedom to use for each shaft. The second question is: How do these discretized shaft models work in the combined system model?

For the sake of example, assume that all the discrete dynamic elements-- inertias J_1, J_2, and J_3, and springs k_1 and k_2 -- have unit parameters. Assume that both shafts are uniform and identical except that shaft 1 is twice the length of shaft 2. Also assume that modal approximations are to be used to discretize the two shafts. Just looking at the shafts, one might reasonably discretize them using twice as many modes for shaft 1 as for shaft 2 since they are identical except for shaft 1 being twice as long. Suppose one uses

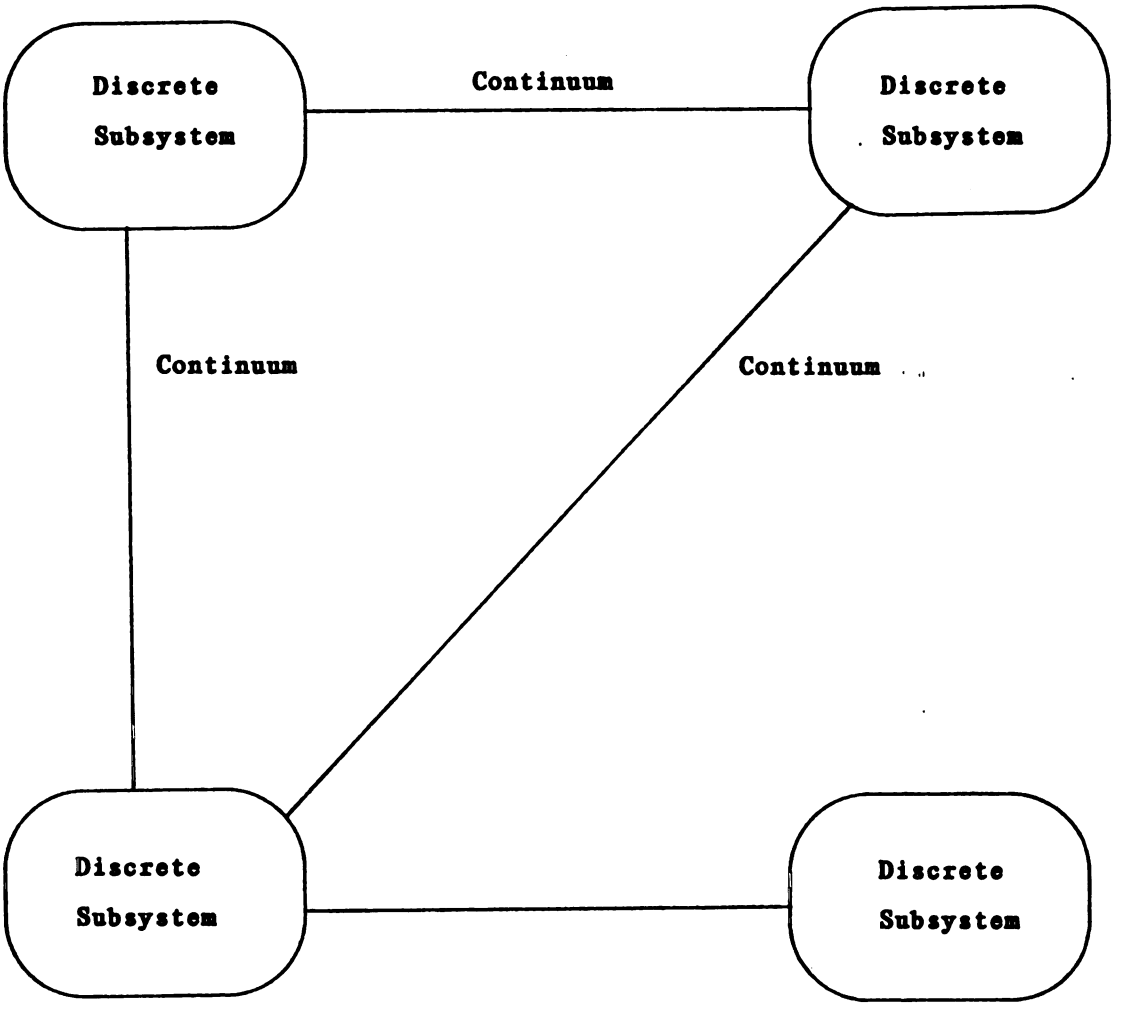

Figure 1.1 Typical Mixed-Structure System

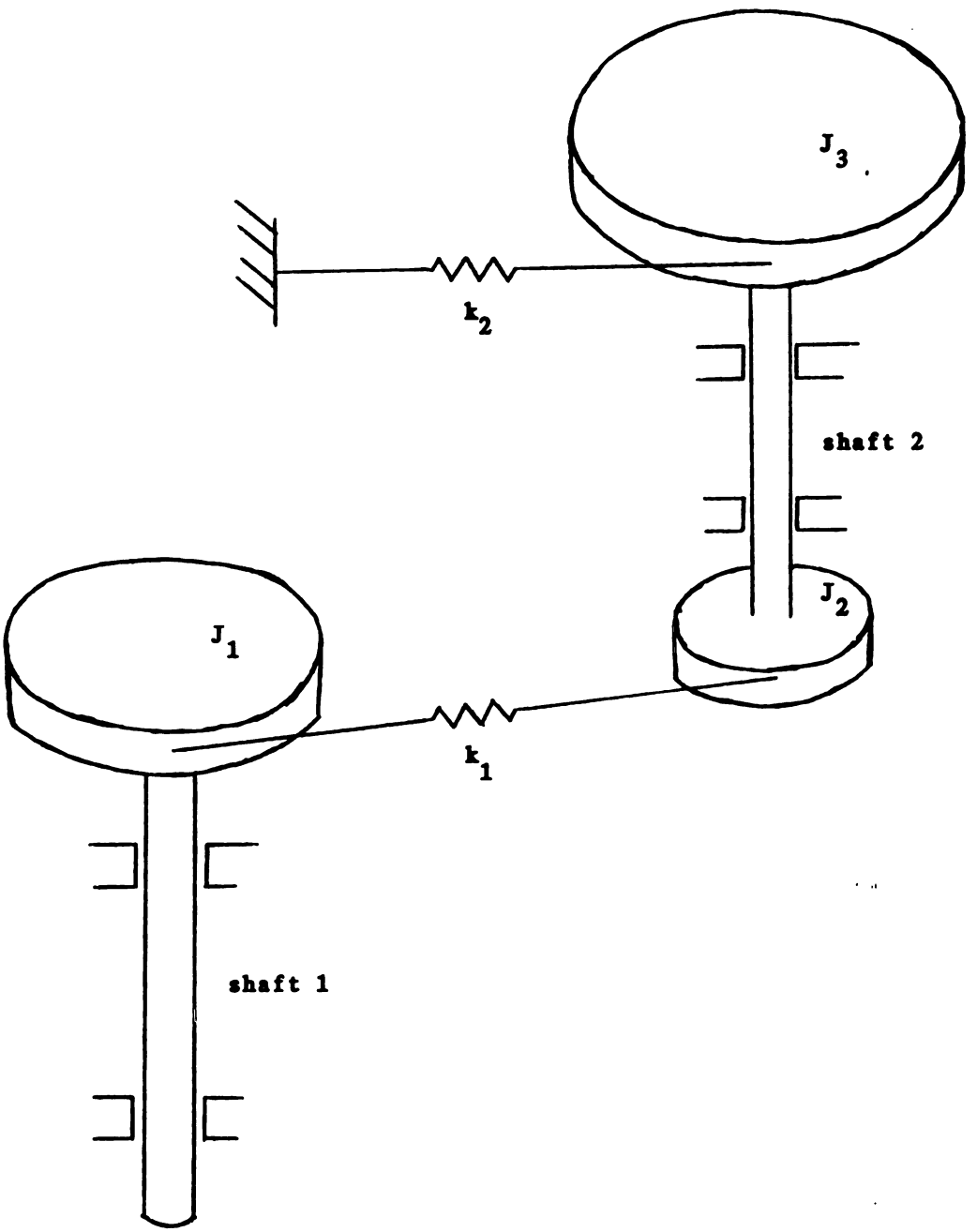

Figure 1.2 Rotational Positioning Mechanism

four modes for shaft 1 and two modes for shaft 2. How well will these shaft models work in the combined system model? What if J_3 and spring k_2 have a frequency near the third mode of shaft 2? How will using only two modes for shaft 2 affect the resulting system model? Assuming that J_3 and spring k_2 have a frequency near the third mode of shaft 2, what if J_3 is much less than or much greater than the inertia of shaft 2? How will using only two modes for shaft 2 affect the quality of the resulting system model? So even if the discretized continuum representations are assumed to be good approximations of the continuum elements, some thought must be given to how the approximations will be interacting with the discrete dynamic elements in the mixed-structure system.

Above it was stated that there is a need to discretize the continuum elements in a mixed-structure system. This need to discretize the continuum elements results from the coupling that exists between the partial differential equations (PDEs) representing the continuum elements and the systems of ordinary differential equations (ODEs) representing the inherently discrete subsystems. As shown in Figure 1.3, the continuum elements in the linear mixed-structure (LMS) system give rise to partial differential equations (PDEs) and boundary conditions (BCs). The discrete subsystems yield ordinary differential equations (ODEs). Because of the physical coupling in the LMS system, variables from the PDE representations appear in the ODEs and lumped parameter variables from the ODEs appear in the boundary conditions, coupling the two types of representations. In a few degenerate cases, some of which are discussed in Timoshenko [1], the behavior of the discrete subsystem

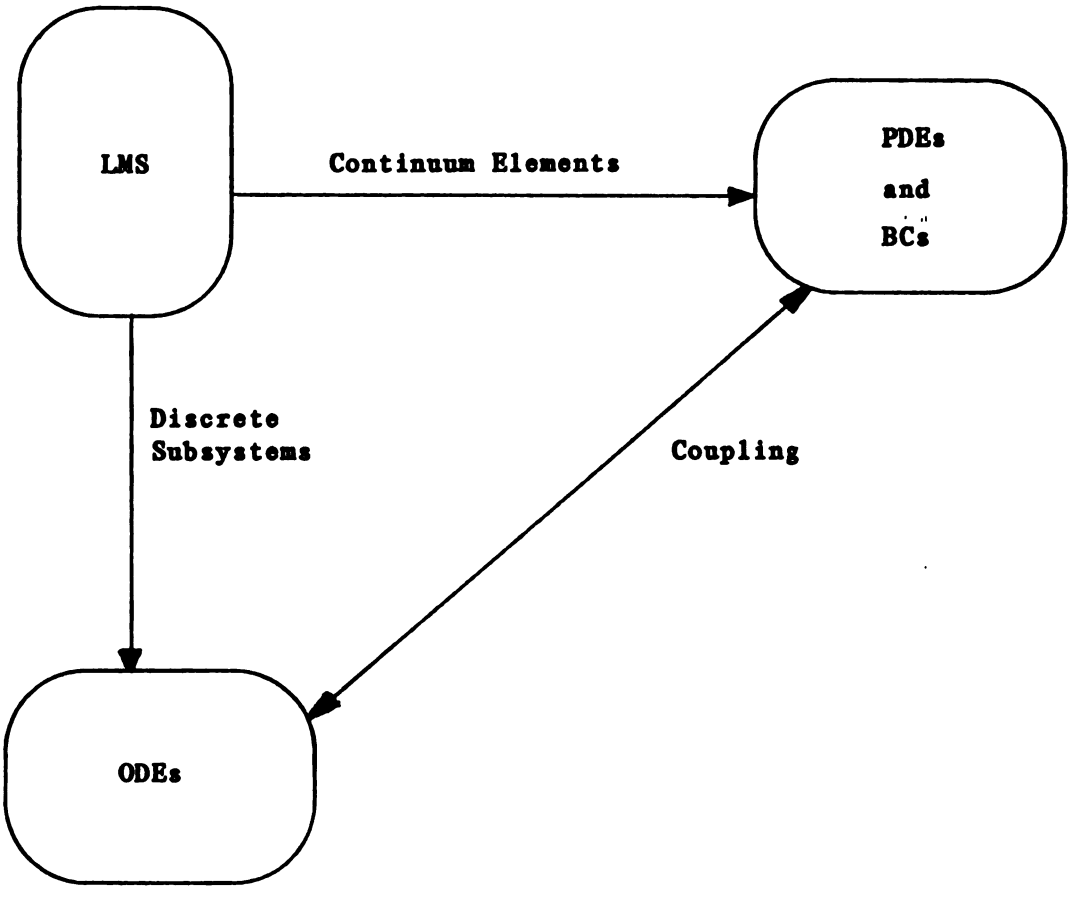

Figure 1.3 Breakdown of LMS System into Mathematical Components

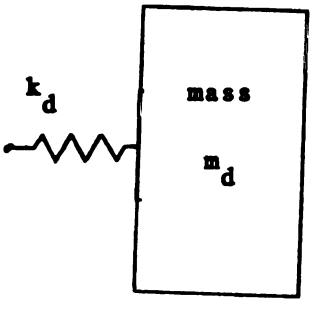

Figure 1.4 Form of Discrete Subsystems

can be described in terms of the coordinates of the continuum element, permitting an analytical solution. But usually an analytical solution is unobtainable. Moreover, the coupling in general has a nontrivial effect on the subsystems and therefore cannot be neglected. Typically what is done is to convert the PDE representations of the continuum elements to ODE representations, so that all the dynamic equations are ODEs.

Several methods are available to convert the PDE representations, including finite element analysis, modal approximation, numerical approximations to the operators, and a physical lumping approach. After a discretization technique has been applied, the discretized representations of the continuum elements and the inherently discrete subsystems are then assembled into an ODE representation of the complete system. To retain sufficient accuracy, large numbers of variables are used to approximate the continuum elements. As a result, the complete system model (hereafter referred to, as in Skelton [2], as the evaluation model) is often too large or expensive to work with directly. In addition, one always has to address the question of "How large is large enough?"

To save computation time in simulations and to facilitate control system design, the evaluation model's size often is reduced in some "optimal" fashion using a model-order reduction procedure. These model order reduction techniques are of two basic types: aggregation and singular perturbation. Both types require three basic elements, namely, an evaluation model, a set of trial models, and a model quality index. As described by Skelton, the model-order reduction problem is fundamentally that of minimizing some model quality index

for all models of a given order that are reduced-order models of a given evaluation model.

Application of either type of model-order reduction procedure is not a simple task. From Aoki [3,4] the aggregation method is seen to be a generalization of the modal approximation procedure developed by Davison [5,6] and others. As such, it typically requires knowledge of the eigenvalues, and often also of the eigenvectors, of the evaluation model. The singular perturbation method does not require the evaluation model eigenvalues and eigenvectors. But it is a nontrivial problem to formulate the system equations in the format required by the theory.

Since the aim of the modelling procedure often is to obtain an accurate system representation of relatively low order, it would be useful in these cases if this representation could be formulated directly, bypassing the formulation of the evaluation model and application of a model-order reduction procedure. Consider, for example, the preliminary stages of the design process. Here the systems engineer quite often has a large number of possible design configurations to choose from. In addition, available computational resources may be limited, prohibiting the formulation and reduction of many evaluation models. Even if computational resources aren't limited, the engineer's time is, so it is always an advantage to reduce the number and size of evaluation models to be considered.

1.2 Research Objectives and Problem Restrictions

The goal of this work is to develop a set of guidelines that will help the designer to directly generate efficient working-order models

for linear mixed-structure systems. With these guidelines the designer:

1. specifies a model quality index,
2. breaks the mixed-structure system into segments having one one continuum element in each segment,
3. distributes the eigenvalues among the segments,
4. chooses the number of spring-mass lumps to be used to discretize the continuum elements by examining results for some prototype cases, and
5. assembles the finite-dimensional model using the results from step 4.

In this work a model quality index based on eigenvalues will be used. To emphasize coupling effects and the coupling paths involved while developing the guidelines, linear mixed-structure systems examined here will have cascade structure with discrete subsystems of the form shown in Figure 1.4. To facilitate comparisons between the evaluation model eigenvalues and the low-order model eigenvalues, work will be limited to conservative systems where the continuum elements are uniform and have both inertia and compliance effects.

So this work will pertain to the modelling of linear mixed-structure systems having the following properties:

1. systems are cascade with one-dimensional dynamics,
2. systems are conservative,
3. continuum elements are uniform with dynamics described by second-order equations of the form:

$$a^2 \partial^2 u/\partial t^2 = \partial^2 u/\partial x^2$$

4. discrete subsystems are of the form shown in Figure 1.4, and
5. the model quality index used is based on eigenvalue errors. In what follows, the particular index used is that the first X eigenvalues are each within Y percent of the corresponding eigenvalues from the evaluation model.

1.3 Dissertation Organization

The remainder of the dissertation is organized as follows. In chapter 2, section 2.1 discusses discretizing methods for the continuum elements and the convergence rate of the method used. In section 2.2, the prototype linear mixed-structure system is examined. A new method for solving the problem analytically is developed, along with a procedure for generating evaluation model eigenvalues from the eigenvalues of low-order models. Unit-parameter uniform cascades and the effect of coupling are discussed in section 2.3. The modelling procedure for direct generation of low-order models is given in chapter 3 along with some application examples. Also discussed in chapter 3 is the eigenvector behavior of these models. In chapter 4 a requirement on the form of the discrete subsystems used in developing the modelling procedure is relaxed, and the usefulness of the procedure in these cases is verified.

2. FACTORS AFFECTING DIRECT GENERATION OF LOW-ORDER MODELS

2.1 Discretizing the Continuum Elements and Eigenvalue Convergence

Having set the evaluation framework, the modelling problem can now be addressed. There are two factors affecting the direct formulation of efficient low-order models. They are the strengths of the couplings between subsystems and the discretization method used for the individual continuum elements.

There are many types of discretization techniques available for representing continuum elements. Each of these techniques has its own particular set of advantages and disadvantages with respect to items of interest such as ease of use, convergence behavior, and complexity of the resulting finite dimensional model. The type of discretization used for the continuum elements in this work will be a physical lumping technique. If one considers the continuum element in Figure 2.1, the discretized model of Figure 2.2 results when physical lumping techniques are applied. In determining the discretized system's parameters, the shaft's elastic modulus E, density ρ, length h, and cross-sectional area A are used to define a static stiffness, $k_s=EA/h$, and the shaft's mass, $m_s=\rho Ah$. Then, in discretizing, the shaft is broken into L spring-mass lumps, with each spring having stiffness $k=k_sL$, and each mass having mass $m=m_s/L$. The resulting eigenvalue problem for the system in Figure 2.2 is:

$$-\omega^2 m[I]x+k_s[K]x=0 \qquad (2\text{-}1)$$

Here ω is the system natural frequency, [I] is the LxL identity matrix,

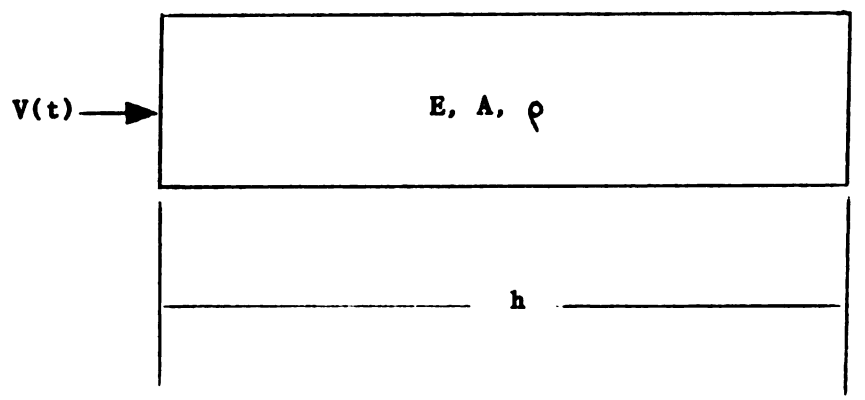

Figure 2.1 Uniform Continuum Element

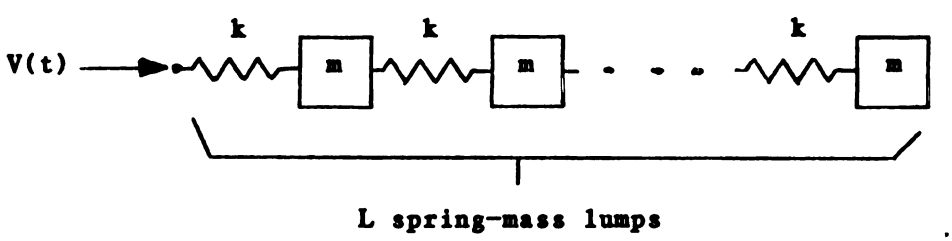

Figure 2.2 Discretized Uniform Continuum Element

x is the vector of displacements, and [K] is the banded stiffness matrix given below.

$$[K]=\begin{bmatrix} 2L & -L & 0 & & & & \\ -L & 2L & -L & 0 & & & \\ 0 & -L & 2L & -L & 0 & & \\ & & \cdot & \cdot & \cdot & & \\ & & & \cdot & \cdot & \cdot & \\ & & & & \cdot & \cdot & \cdot \\ & & & & & -L & 2L & -L \\ & & & & & 0 & -L & L \end{bmatrix} \qquad (2\text{-}2)$$

This system of equations is the same as the finite difference formulation given below in equations (2-3) and (2-4). That is, if the values of the index n are substituted in (2-3) and the boundary conditions (2-4) applied, the system of equations in (2-1) results.

$$-EAL(\theta_{n+1}-2\theta_n+\theta_{n-1})/h = \omega^2\rho Ah\theta_n/L \qquad (2\text{-}3)$$

$$\theta_0=0 \qquad (\theta_{L+1}-\theta_L)/(h/L)=0 \qquad (2\text{-}4)$$

Solving the finite difference equation for ω (see Appendix A) and using the known solution $\bar{\omega}$ of the continuum boundary value problem, one can generate the following expression for the eigenvalue errors in the discrete approximation.

$$((\omega-\bar{\omega})/\bar{\omega})_j = (4L/(2j-1)\pi)\sin[(2j-1)\pi/2(2L+1)] - 1 \qquad (2\text{-}5)$$

$$j=1,2, \ . \ . \ . \ ,L$$

Performing a Taylor series expansion of the sine term in equation (2-5) above results in the error expression below.

$$(\omega-\bar{\omega}/\bar{\omega})_j = -1/(2L+1)- \ . \ . \ . \qquad (2-6)$$

So the convergence of the physical lumping discretization is of the order (1/(2L+1)), or approximately order (1/2L) for large L.

2.2 The Prototype Linear Mixed-Structure System

2.2.1 Analytical Solutions

Define the system of Figure 2.3 to be the prototype linear mixed-structure system. Analytical solutions for this case are more difficult to obtain than for the system of Figure 2.4, whose solution is discussed in Timoshenko. The difficulty in solving the prototype linear mixed-structure system results from the appearance of the independent coordinate y describing the position of the discrete mass. Jacquot and Soedel [7] and Young [8] have found a solution to this problem. In their approach, the discrete spring-mass subsystem is replaced by a harmonic forcing function. Assuming that the eigenvalues ω_i and eigenfunctions $\phi_i(x)$ of the shaft are known, the forced solution can be obtained in terms of eigenfunction expansions. Using the displacement impedance for the spring-mass system at the point of attachment, the forced solution can then be viewed as a solution to the prototype linear mixed-structure system. From this one obtains the frequency relation:

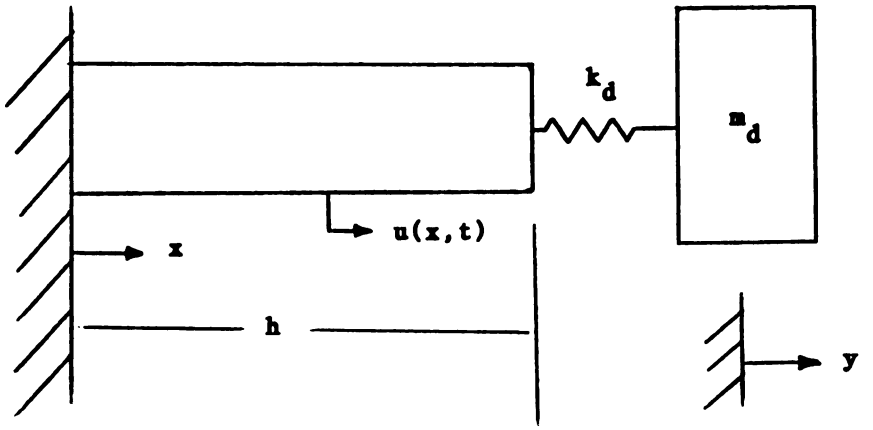

Figure 2.3 Prototype LMS System

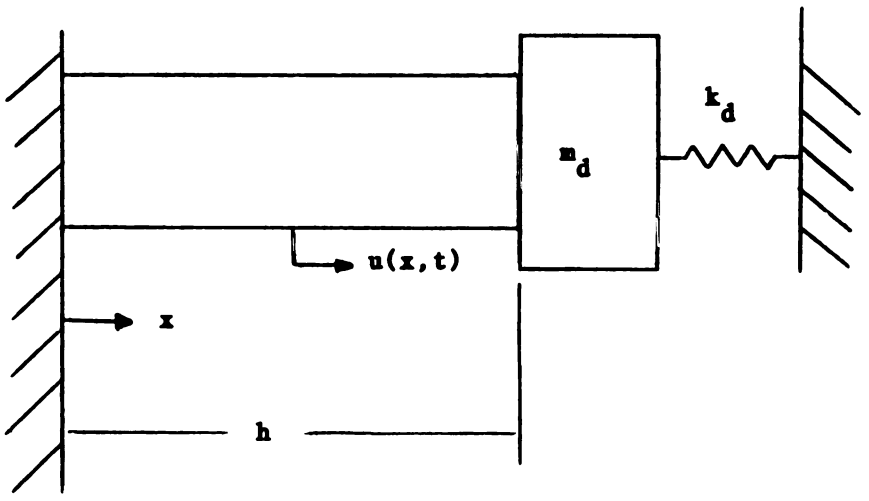

Figure 2.4 One-Segment LMS System with Dependent Mass Element

$$1-k_d m_d \omega^2/(k_d-m_d\omega^2)\sum_{i=1}^{\infty}\phi_i^2(h)/\rho A\|\phi_i\|^2(\omega_i^2-\omega^2)=0 \qquad (2\text{-}7)$$

Here ω is the natural frequency of the prototype LMS system, ω_i and $\phi_i(x)$ are the eigenvalues and eigenfunctions of the shaft, and k_d and m_d are the stiffness and mass of the discrete subsystem.

In this work an alternative solution to the prototype linear mixed-structure problem is developed that treats the boundary value problem directly.(See Appendix B). For the prototype linear mixed-structure system, the boundary value problem is:

$$\partial^2 u/\partial x^2=(1/a^2)\partial^2 u/\partial t^2 \qquad a^2=E/\rho \qquad (2\text{-}8)$$

$$m_d y''(t)=-k_d(y(t)-u(h,t)) \qquad (2\text{-}9)$$

$$u(0,t)=0 \qquad EA(\partial u/\partial x)\Big|_{x=h}=k_d(y(t)-u(h,t)) \qquad (2\text{-}10)$$

At a natural frequency of the system, the motions are synchronous and all amplitudes can be expressed in terms of the amplitude of one of the points. So with the assumption that $y(t)=cu(h,t)$, c constant, the coordinate y can be removed from the problem. Solving using the standard separation of variables technique results in the frequency relation:

$$\omega=(ak_d/EA)(\omega^2 m_d/(k_d-\omega^2 m_d))\tan(\omega h/a) \qquad (2\text{-}11)$$

Contrasting the two solutions one can see that the direct solution to the boundary value problem has some advantages over the

solution from Jacquot and Soedel. In particular, one need not know the eigenvalues and eigenfunctions of the shaft. Both equations (2-7) and (2-11) require an iterative solution technique. But equation (2-7) also requires that one truncate the infinite series before beginning any computation for the natural frequencies. This is a level of approximation not required in equation (2-11). The two solutions were compared for a prototype system with elastic modulus E=100, density ρ=100, cross-sectional area A=0.01, shaft length h=1.0, and discrete subsystem parameters k_d=1 and m_d=1. For the shaft, the eigenvalues and eigenfunctions are:

$$\omega_i = i\pi/2 \qquad \phi_i(x) = \sin(i\pi x) \qquad i=1,3,5, \ldots \tag{2-12}$$

Keeping 10000 modes in equation (2-7), the results shown in Table 2.1 below were obtained.

Table 2.1 Comparison of Analytical Eigenvalue Solutions

Eigenvalue	Solution from (2-7)	Solution from (2-11)
1	0.6762	0.6762
2	2.117	2.117
3	4.921	4.921
4	7.980	7.980
5	11.086	11.086

One can see that the solution technique developed here yields results that agree with those derived from Jacquot and Soedel's technique. The primary use of these analytical solutions in this work is as a

check for the procedure used to generate the evaluation model eigenvalues for linear mixed-structure systems.

2.2.2 The Discretized Prototype Problem and Evaluation Model Eigenvalues

Now consider the discretized prototype linear mixed-structure system in Figure 2.5. The elements labelled k and m are derived from the continuum, while k_d and m_d denote the discrete subsystem. The eigenvalue problem for this system is:

$$-\omega^2[M]x+[K]x=0 \tag{2-13}$$

$$[M]=\begin{bmatrix} m & 0 & & & & & \\ 0 & m & 0 & & & & \\ & 0 & m & 0 & & & \\ & & \cdot & \cdot & \cdot & & \\ & & & \cdot & \cdot & \cdot & \\ & & & & \cdot & \cdot & \cdot \\ & & & & & 0 & m & 0 \\ & & & & & & 0 & m_d \end{bmatrix} \tag{2-14}$$

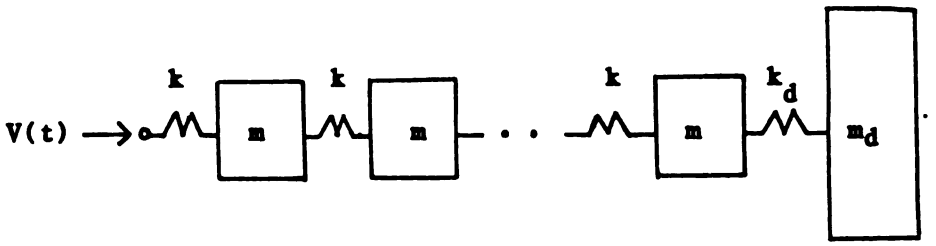

Figure 2.5 Discretized Prototype LMS System

$$[K]=\begin{bmatrix} 2k & -k & 0 & & & & \\ -k & 2k & -k & 0 & & & \\ 0 & -k & 2k & -k & 0 & & \\ & & \cdot & \cdot & \cdot & & \\ & & & \cdot & \cdot & \cdot & \\ & & & & \cdot & \cdot & \cdot \\ & & & & -k & (k+k_d) & -k_d \\ & & & & 0 & -k_d & k_d \end{bmatrix} \qquad (2\text{-}15)$$

Here $k=k_sL$ and $m=m_s/L$. Premultiplying by $[M]^{-1}$ gives the equivalent expression:

$$-\omega^2[I]x+[A]x=0 \qquad (2\text{-}16)$$

Where $[A]=[M]^{-1}[K]$. (2-17)

$$[A]=k_s/m_s\begin{bmatrix} 2L^2 & -L^2 & & & & & \\ -L^2 & 2L^2 & -L^2 & & & & \\ & \cdot & \cdot & \cdot & & & \\ & & \cdot & \cdot & \cdot & & \\ & & & \cdot & \cdot & \cdot & \\ & & & & -L^2 & (k_d/k_s+L)L & -Lk_d/k_s \\ & & & & 0 & -k_dm_s/k_sm_d & k_dm_s/k_sm_d \end{bmatrix} \qquad (2\text{-}18)$$

One can see from (2-18) above that the parameters of interest in the discretized problem are the stiffness ratio k_d/k_s, the mass ratio m_s/m_d, and the number of spring-mass lumps, L.

If one lets L go to infinity, the eigenvalues of the discretized problem will converge to the eigenvalues from the analytical solutions discussed above. For a physical lumping discretization of the continuum element, it was shown previously that the convergence was of order (1/(2L+1)). Making explicit use of the rate of convergence, a least-squares method was used to generate the evaluation model eigenvalues without solving a very large eigenvalue problem. Let

$$\omega_j = C_0 + C_1/(2L+1) + C_2/(2L+1)^2 + C_3/(2L+1)^3 \qquad (2\text{-}19)$$

Here C_0, C_1, C_2, and C_3 are constants to be determined, L is the number of spring-mass lumps used to discretize the continuum, and ω_j is the corresponding eigenvalue for a given L. If a number of relatively low-order models are run and a least-squares method is applied using equation (2-19), the constants C_0, C_1, C_2, and C_3 can be determined. Note that C_0 will correspond to the evaluation model eigenvalue for a given sequence of eigenvalues $\{\omega_j^{(L)}\}_{j=\text{constant}}$. To check this procedure, a number of low-order problems were run for the example above, and a least-squares curvefit was applied using equation (2-19). Consider the second eigenvalue of the system. To apply the curvefit procedure, 11 relatively low-order models were run, using between 3 and 80 spring-mass lumps to approximate the shaft. Applying a least-squares fit of equation (2-19) to the data for the second eigenvalue gives:

$C_0=4.921$ $C_1=-4.495$ $C_2=-21.469$ $C_3=20.519$

Figure 2.6 shows a plot of equation (2-19) using these parameters through the eigenvalue data. Table 2.2 below compares the results obtained from the curvefit technique with the analytical solutions from equation (2-7).The results from the least-squares curvefit technique agree with the analytical solutions, supporting the idea that the convergence for the linear mixed-structure system is the same type as it is for the continuum element when physical lumping is used to discretize. So in future examples the evaluation model eigenvalues will be generated using this curvefit technique.

Table 2.2 Comparison of Curvefit Results and Analytical Solutions

Eigenvalue	Solution from Curvefit	Solution from (2-7)
1	0.6762	0.6762
2	2.117	2.117
3	4.921	4.921
4	7.980	7.980
5	11.086	11.086

2.3 Unit-Parameter Uniform Cascades

2.3.1 Clustering Behavior of Eigenvalues

Having dealt with the question of how to discretize the continuum elements, the other main point to address is the coupling effect between subsystems. In order to examine coupling effects, a study was run using the sequence of unit-parameter uniform cascades shown in Figure 2.7. For all the continuum elements, the parameters were $k_s=1$, $m_s=1$. And for all the discrete subsystems, they were $k_d=1$, $m_d=1$.

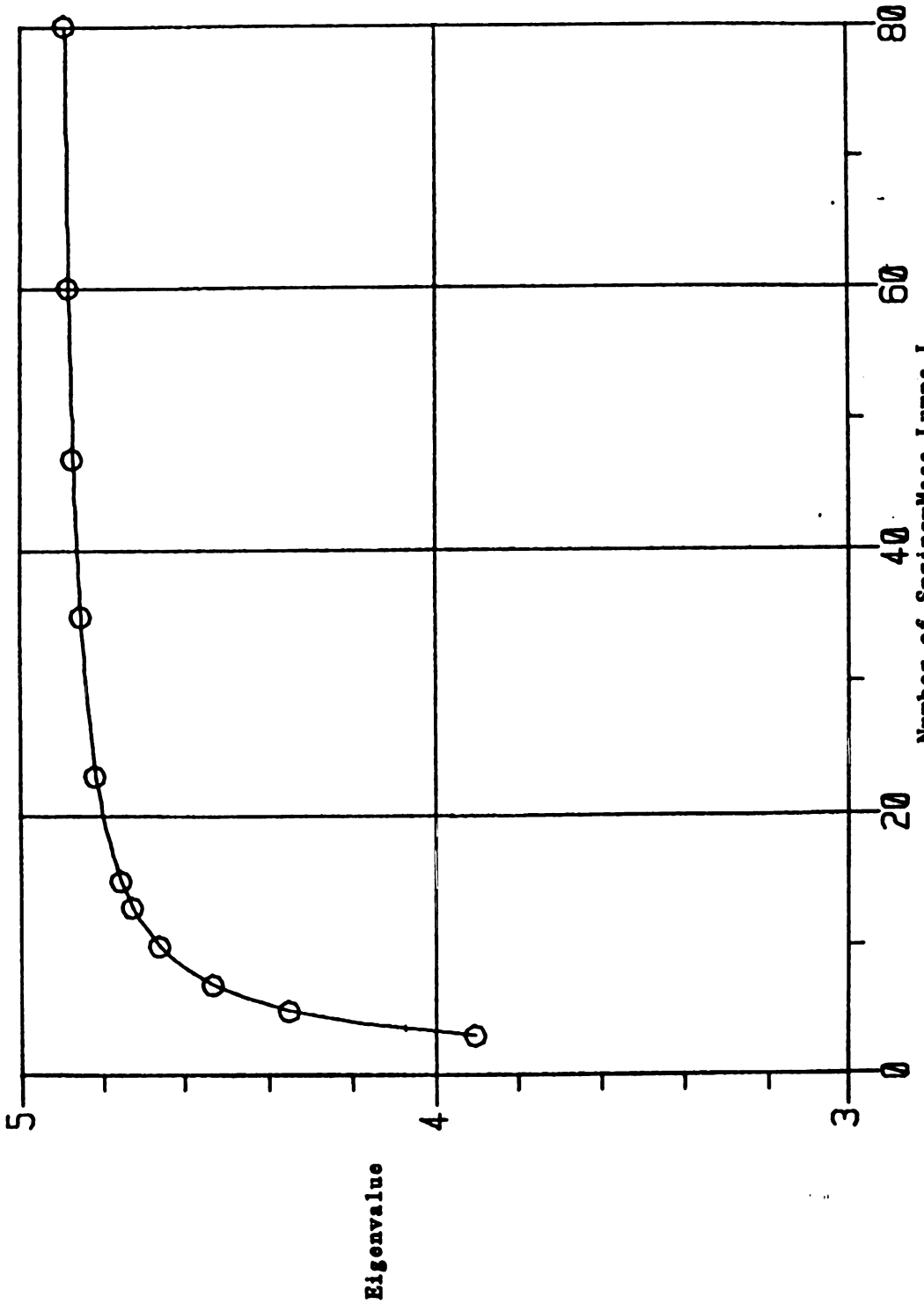

Figure 2.6 Least-Squares Curvefit to Eigenvalue Data

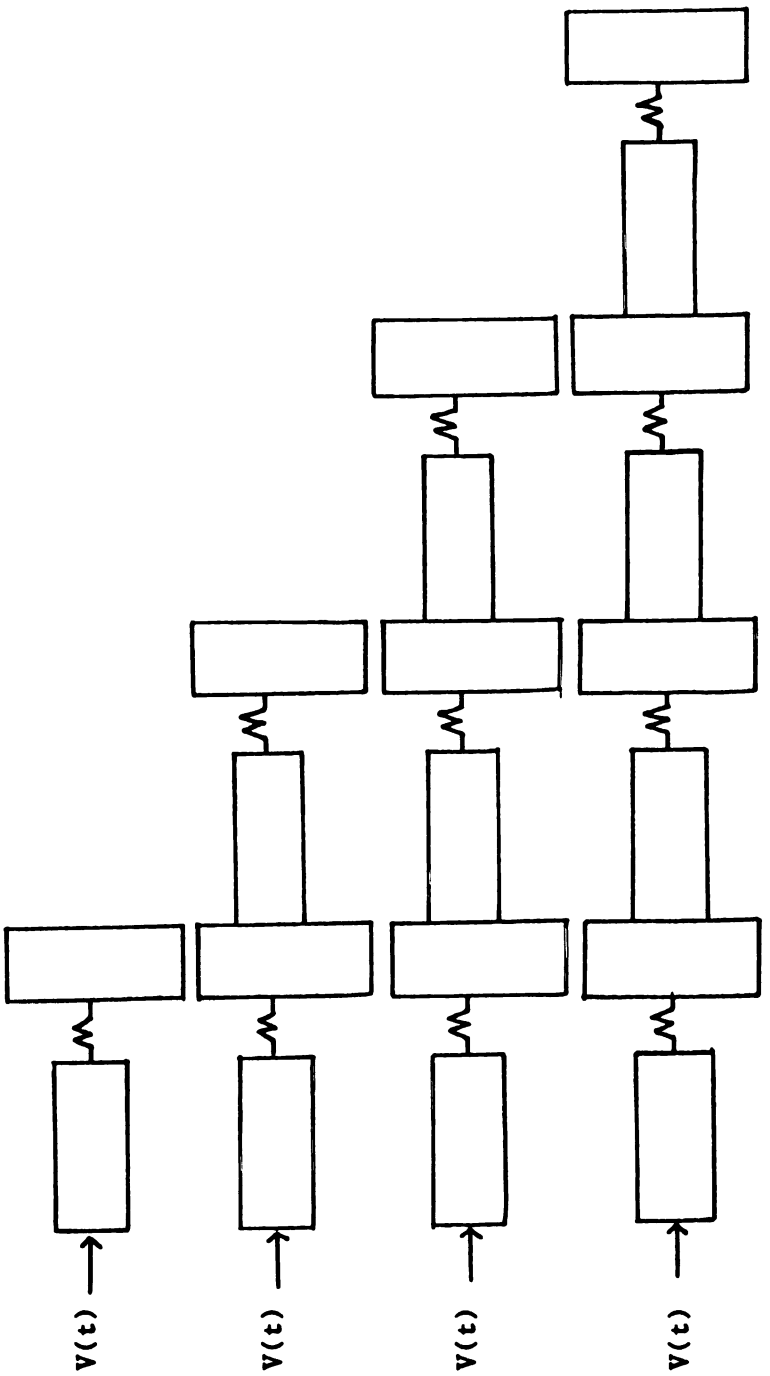

Figure 2.7 Cascade Systems of Increasing Size

Consider for example, the two-segment cascade shown in Figure 2.8. Since the two uncoupled segments in Figure 2.9 are identical, they have identical spectra. Then when the segments are coupled, as in Figure 2.8, one expects the coupling to perturb the eigenvalues somewhat. But because the uncoupled segments have identical spectra, one would intuitively expect the coupled system spectrum to have clusters of eigenvalues, with two eigenvalues to a cluster. Similarly, one would expect that as the number of segments in the uniform cascade changes, the number of eigenvalues in a cluster changes such that the number of eigenvalues in a cluster is the same as the number of segments in the cascade. As an example, consider the three-segment case. With L=15 for each shaft, the first 15 eigenvalues are those given in Table 2.3 below.

Table 2.3 Eigenvalues for the 3-Segment Unit-Parameter Uniform Cascade

0.2498	1.9863	4.7455	7.6415	10.503
0.7277	2.3269	4.9142	7.7489	10.579
1.1013	2.5446	4.9883	7.7797	10.594

Near the low end of the spectrum, some clustering is evident but the width of the cluster is relatively large. As the frequency increases through the spectrum the width of the clusters decreases. Using the following theorem from Crawford [9], a bound can be obtained on the perturbation introduced by the coupling.

1. Theorem: Let M_u, K_u, F, and H be real symmetric nxn matrices with M_u and (M_u+F) positive definite. Let

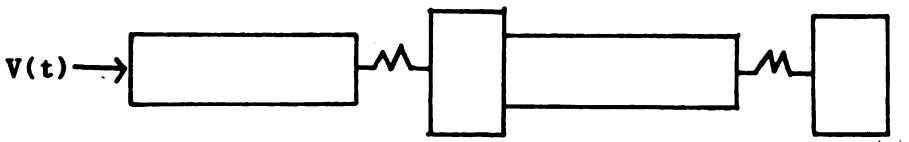

Figure 2.8 Two-Segment Cascade

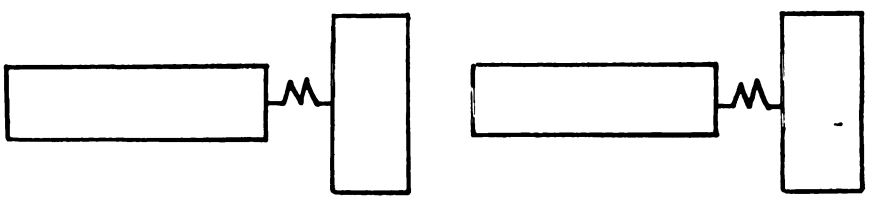

Figure 2.9 Two Identical One-Segments

$\{\lambda_j\}=\lambda(M_u,K_u)$ and $\{\bar{\lambda}_j\}=\lambda(M_u+F,K_u+H)$

with $\{\lambda_j\}$, $\{\bar{\lambda}_j\}$ numbered in increasing order. Then

$$\left|\lambda_j-\bar{\lambda}_j\right| < \left\|(M_u+F)^{-1}\right\|\left(\left\|F\right\|\left|\lambda_j\right| + \left\|H\right\|\right) \quad j=1,\ldots,n \tag{2-20}$$

For the cascade problem with physical lumping discretizations of the continuum elements:

$$F=0 \qquad \lambda_j=\omega_j^2>0 \qquad \bar{\lambda}_j=\bar{\omega}_j^2>0$$

Then from the theorem above,

$$\left|\omega_j^2-\bar{\omega}_j^2\right| < \left\|M_u^{-1}\right\|\left\|H\right\| \tag{2-21}$$

So the absolute perturbation in any eigenvalue is bounded by a constant $\left\|M_u^{-1}\right\|\left\|H\right\|$. More importantly, if one considers the relative perturbation,

$$\left|(\omega_j^2-\bar{\omega}_j^2)/\omega_j^2\right| < \left\|M_u^{-1}\right\|\left\|H\right\|/\omega_j^2 \tag{2-22}$$

it is clear that as the frequency increases the effect of the coupling decreases.

2.3.2 Average Eigenvalues and Error Behavior

In order to compare the systems of Figure 2.7 directly, average eigenvalues were defined for each system. The average eigenvalues are defined to be the averages of the eigenvalues in the clusters. With this concept, the unit parameter uniform cascades can be compared directly.

For each of the systems of Figure 2.7 a large number of discretized models was evaluated. The average eigenvalues were determined and the errors, compared to the average eigenvalues for the evaluation model, were computed and tabulated. These results in Table 2.4 show that the errors in the average eigenvalues are nearly stationary. At each location in the table, a set of four numbers appears. From top down in a set, these four numbers are the magnitudes of the errors in the average eigenvalues for the one, two, three, and four-segment models respectively. Consider, for example, the fourth average eigenvalue when the number of lumps per shaft L is 6. The errors for the one, two, three, and four-segment cases are 13.22, 13.28, 13.30, 13.31 percent respectively. Also, in examining the table, it is clear that any increases in errors between the one-segment case and the multi-segment cases are less than one percent. From this it can be concluded that the cascade coupling has little effect on the eigenvalue errors. Because the coupling has little effect, large cascades can be viewed as assemblies of 1-segment cascades. Discretization can be performed on each segment separately to meet the model quality index.

In order to apply the procedure suggested above, errors for the 1-segment case must be well documented. Recall that in section 2.2

Table 2.4 Average Eigenvalue Errors for Unit-Parameter Uniform Cascades

Eigenvalue	Number of Lumps per Shaft L												
	2	3	4	5	6	7	8	9	10	11	12	13	14
1	3.83	2.44	1.78	1.40	1.16	0.98	0.85	0.75	0.67	0.61	0.56	0.51	0.47
	0.49	0.56	0.50	0.43	0.38	0.34	0.32	0.28	0.26	0.24	0.22	0.21	0.20
	1.77	1.37	1.09	0.89	0.76	0.66	0.58	0.52	0.47	0.43	0.40	0.37	0.34
	2.46	1.84	1.47	1.22	1.05	0.93	0.83	0.76	0.70	0.65	0.60	0.57	0.53
2	13.14	9.00	6.81	5.47	4.57	3.92	3.43	3.05	2.74	2.49	2.29	2.11	1.96
	13.30	8.85	6.59	5.23	4.32	3.68	3.20	2.83	2.54	2.30	2.10	1.93	1.78
	13.33	8.80	6.52	5.16	4.26	3.62	3.15	2.79	2.49	2.26	2.06	1.90	1.75
	13.32	8.75	6.45	5.10	4.21	3.58	3.11	2.74	2.45	2.22	2.03	1.86	1.72
3	31.98	20.63	14.91	11.55	9.38	7.87	6.77	5.92	5.26	4.73	4.30	3.93	3.62
	32.38	20.73	14.88	11.47	9.27	7.75	6.64	5.80	5.14	4.62	4.18	3.82	3.52
	32.52	20.77	14.88	11.45	9.25	7.73	6.62	5.78	5.12	4.59	4.16	3.80	3.45
	32.59	20.79	14.88	11.45	9.24	7.71	6.60	5.76	5.10	4.58	4.14	3.79	3.48
4		31.72	22.25	16.73	13.22	10.82	9.11	7.82	6.83	6.05	5.42	4.90	4.46
		32.03	22.44	16.84	13.28	10.85	9.12	7.82	6.82	6.03	5.40	4.87	4.43
		32.13	22.50	16.87	13.30	10.86	9.12	7.82	6.82	6.03	5.39	4.86	4.42
		32.18	22.53	16.89	13.31	10.87	9.12	7.82	6.82	6.02	5.38	4.86	4.42
5			32.00	23.75	18.49	14.91	12.38	10.50	9.07	7.95	7.05	6.31	5.71
			32.12	23.81	18.49	14.89	12.32	10.43	8.98	7.85	6.94	6.21	5.60
			32.22	23.90	18.57	14.95	12.38	10.48	9.04	7.90	6.99	6.25	5.65
			32.27	23.94	18.60	14.99	12.41	10.51	9.06	7.93	7.02	6.28	5.67
6				32.32	24.97	19.96	16.40	13.77	11.77	10.21	8.98	7.97	7.15
				32.34	24.95	19.91	16.32	13.68	11.66	10.10	8.85	7.84	7.01
				32.33	24.93	19.88	16.28	13.62	11.61	10.04	8.79	7.77	6.94
				32.47	25.08	20.03	16.43	13.78	11.76	10.20	8.95	7.93	7.10
7					32.70	26.07	21.34	17.83	15.16	13.09	11.44	10.11	9.02
					32.60	25.95	21.19	17.66	14.98	12.89	11.23	9.89	8.79
					32.60	25.94	21.16	17.63	14.95	12.85	11.19	9.85	8.75
					32.60	25.94	21.16	17.62	14.93	12.84	11.18	9.83	8.73

At each location on the table, a set of four numbers appears. From top down in a set, these four numbers are the magnitudes of the errors in the average eigenvalues for the one, two, three, and four-segment models respectively.

Table 2.4 Average Eigenvalue Errors for Unit-Parameter Uniform Cascades

	Number of Lumps per Shaft L												
Eigenvalue	2	3	4	5	6	7	8	9	10	11	12	13	14
1	3.83	2.44	1.78	1.40	1.16	0.98	0.85	0.75	0.67	0.61	0.56	0.51	0.47
	0.49	0.56	0.50	0.43	0.38	0.34	0.32	0.28	0.26	0.24	0.22	0.21	0.20
	1.77	1.37	1.09	0.89	0.76	0.66	0.58	0.52	0.47	0.43	0.40	0.37	0.34
	2.46	1.84	1.47	1.22	1.05	0.93	0.83	0.76	0.70	0.65	0.60	0.57	0.53
2	13.14	9.00	6.81	5.47	4.57	3.92	3.43	3.05	2.74	2.49	2.29	2.11	1.96
	13.30	8.85	6.59	5.23	4.32	3.68	3.20	2.83	2.54	2.30	2.10	1.93	1.78
	13.33	8.80	6.52	5.16	4.26	3.62	3.15	2.79	2.49	2.26	2.06	1.90	1.75
	13.32	8.75	6.45	5.10	4.21	3.58	3.11	2.74	2.45	2.22	2.03	1.86	1.72
3	31.98	20.63	14.91	11.55	9.38	7.87	6.77	5.92	5.26	4.73	4.30	3.93	3.62
	32.38	20.73	14.88	11.47	9.27	7.75	6.64	5.80	5.14	4.62	4.18	3.82	3.52
	32.52	20.77	14.88	11.45	9.25	7.73	6.62	5.78	5.12	4.59	4.16	3.80	3.45
	32.59	20.79	14.88	11.45	9.24	7.71	6.60	5.76	5.10	4.58	4.14	3.79	3.48
4		31.72	22.25	16.73	13.22	10.82	9.11	7.82	6.83	6.05	5.42	4.90	4.46
		32.03	22.44	16.84	13.28	10.85	9.12	7.82	6.82	6.03	5.40	4.87	4.43
		32.13	22.50	16.87	13.30	10.86	9.12	7.82	6.82	6.03	5.39	4.86	4.42
		32.18	22.53	16.89	13.31	10.87	9.12	7.82	6.82	6.02	5.38	4.86	4.42
5			32.00	23.75	18.49	14.91	12.38	10.50	9.07	7.95	7.05	6.31	5.71
			32.12	23.81	18.49	14.89	12.32	10.43	8.98	7.85	6.94	6.21	5.60
			32.22	23.90	18.57	14.95	12.38	10.48	9.04	7.90	6.99	6.25	5.65
			32.27	23.94	18.60	14.99	12.41	10.51	9.06	7.93	7.02	6.28	5.67
6				32.32	24.97	19.96	16.40	13.77	11.77	10.21	8.98	7.97	7.15
				32.34	24.95	19.91	16.32	13.68	11.66	10.10	8.85	7.84	7.01
				32.33	24.93	19.88	16.28	13.62	11.61	10.04	8.79	7.77	6.94
				32.47	25.08	20.03	16.43	13.78	11.76	10.20	8.95	7.93	7.10
7					32.70	26.07	21.34	17.83	15.16	13.09	11.44	10.11	9.02
					32.60	25.95	21.19	17.66	14.98	12.89	11.23	9.89	8.79
					32.60	25.94	21.16	17.63	14.95	12.85	11.19	9.85	8.75
					32.60	25.94	21.16	17.62	14.93	12.84	11.18	9.83	8.73

At each location on the table, a set of four numbers appears. From top down in a set, these four numbers are the magnitudes of the errors in the average eigenvalues for the one, two, three, and four-segment models respectively.

the key parameters in the discretized 1-segment (prototype) linear mixed-structure system were determined to be k_d/k_s, m_s/m_d, and L. The 1-segment case was studied for a number of variations of these parameters and the error results were tabulated using tables of the form shown in Figure 2.10.(See Appendix C). In examining these tables, keep in mind that L is a discrete variable, but the stiffness ratio k_d/k_s and the mass ratio m_s/m_d are continuous variables.

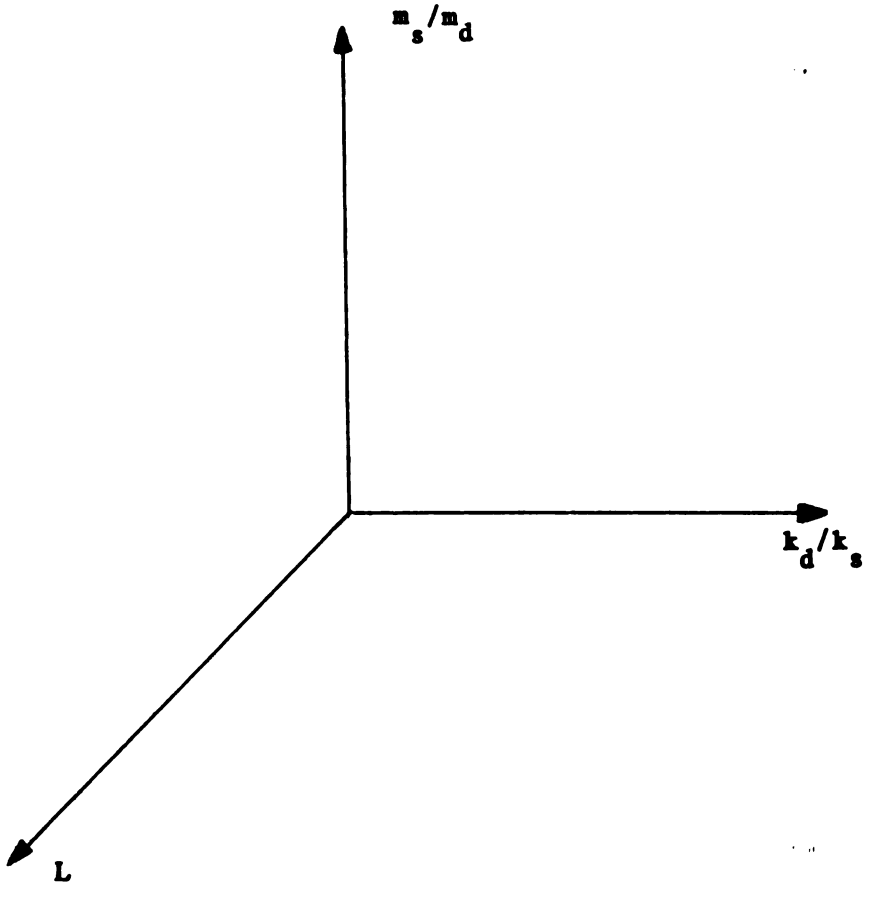

Figure 2.10 Format of the One-Segment Error Tables

3. NON-UNIFORM CASCADE MODELLING PROCEDURE

3.1 Description of Procedure

Having examined the factors affecting direct generation of efficient low-order models, a design procedure can now be given. The following procedure is applicable to any linear cascade system having the properties given in Chapter 1.

1. Define a model quality index based on eigenvalue errors. This index will be used for determining the accuracy of the low-order model. In the examples that follow, the index used is that the first X eigenvalues each have less than Y percent error.
2. Account for any coupling effects that occur when joining segments by reducing the acceptable eigenvalue error Y by one percent. $Y'=Y-1$.
3. The X system eigenvalues of interest are now distributed among the segments in the cascade. Say the cascade has M segments. Let N_i be the number of eigenvalues associated with segment i, $1 \leq i \leq M$. For each segment define:

$$\Delta_i=(\pi/2h_i)\sqrt{E_i/\rho_i} \qquad (3\text{-}1)$$

Divide each Δ_i by the largest of the Δ_i, call it Δ_k. Then for each eigenvalue associated with segment k, segment i has (Δ_k/Δ_i) eigenvalues associated with it. Solve the following for the N_i. If any of the N_i contain a fractional part, round that N_i up to the next integer.

$$N_i=(\Delta_k/\Delta_i)N_k \qquad i=1,2,\ .\ .\ .\ ,M \qquad (3\text{-}2)$$

$$X=N_1+N_2+\ .\ .\ .\ +N_M \qquad (3\text{-}3)$$

4. Consider each segment as a separate problem where the model quality index is that the first N (rounded up to the nearest integer) eigenvalues each have less than Y' percent error. Determine k_d/k_s, and m_s/m_d for each segment. Check the first N error tables in Appendix C to find the number of lumps L needed for each segment to meet the error criterion Y'.
5. Assemble the low-order system model.

3.2 Application Examples.

Several examples are given here to illustrate the application of the procedure to a number of different cascade systems of increasing generality. Examples 1,2, and 3 have the system configuration shown in Figure 3.1.

Example One: Both shafts are identical.

The parameters for the two segments are given in Table 3.1 below.

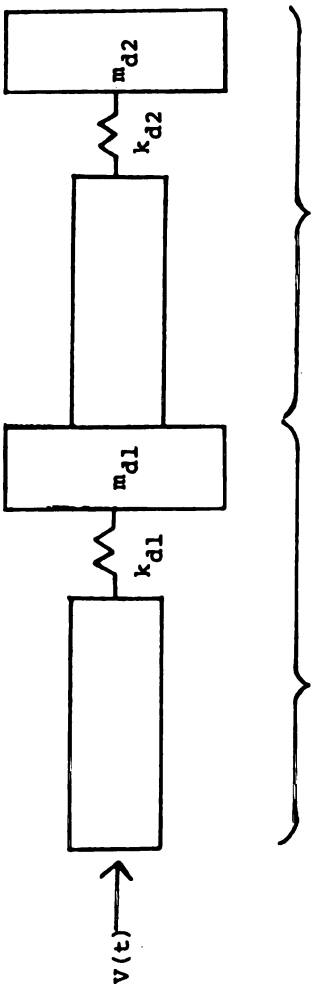

Figure 3.1 Form of Cascade System for Examples 1, 2, and 3

Figure 3.2 Low-Order Model for Example 1

Table 3.1 Parameters for Example 1

	Elastic Modulus	Density	Length	Area	k_s	m_s
segment 1	100	100	1.0	0.01	1.0	1.0
segment 2	100	100	1.0	0.01	1.0	1.0

	k_d	m_d	k_d/k_s	m_s/m_d
segment 1	16.0	1.0	16.0	1.0
segment 2	1.0	1.0	1.0	1.0

Applying the Modelling Procedure:

1. Say that one wants the first 6 eigenvalues each with less than 10 percent error.

2. Account for coupling effects by reducing the acceptable error by 1 percent. Y'=10-1=9.

3. Distribute the eigenvalues among the segments.

$$\Delta_1=(\pi/2h_1)\sqrt{E_1/\rho_1}=(\pi/2)\sqrt{100/100}=\pi/2$$

$$\Delta_2=(\pi/2h_2)\sqrt{E_2/\rho_2}=(\pi/2)\sqrt{100/100}=\pi/2$$

$$N_1=(\Delta_2/\Delta_1)N_2$$

$$N_1=((\pi/2)/(\pi/2))N_2=N_2$$

$$X=N_1+N_2$$

$$6=2N_2 \rightarrow N_2=3 \quad N_1=3$$

4. $N_1=N_2=3$, so use the tables for the first three eigenvalues for both segments. Looking in the 1-segment error tables with the mass and stiffness ratios from Table 3.1 above gives L1=4, L2=7. The low-order system model with L1=4 and L2=7 was assembled(see Figure 3.2), and the eigenvalue simulation run. From the results in Table 3.2, it is clear that the requirements of the model quality index have been met.

Table 3.2 Eigenvalue Data for Example 1

Eigenvalue	L1=4 L2=7	Evaluation Model	Percent Error
1	0.4476	0.4548	-1.58
2	1.0321	1.0419	-0.94
3	2.2337	2.3357	-4.36
4	3.1782	3.2644	-2.64
5	4.6767	5.0935	-8.18
6	5.5759	6.0834	-8.34

Note that if the discretization of the continuum elements was based on the parameters of the continuum elements alone, the same number of variables would be used on each shaft since they are identical. For comparison purposes, the simulation was also run using the same number of lumps on each shaft, with L1=L2=6. The results of the simulation are as follows.

Table 3.3 Eigenvalue Data for Example 1 when Shafts have Identical Discretizations

Eigenvalue	L1=6 L2=6	Percent Error
1	0.4484	-1.40
2	1.0416	-0.03
3	2.2264	-4.68
4	3.2237	-1.25
5	4.6156	-9.38
6	5.8481	-3.87

The results here also meet the model quality index although the maximum error is higher than when the procedure is followed. But one important thing to note here is the selection of the number of lumps to use. Six lumps were used for L1 and L2 so that the total number of lumps used would be nearly the same for the two simulations. But choosing L1=L2 implies that the discrete subsystems do not affect the eigenvalue errors. So the number of lumps to use would be determined by equation (2-5). Using this relation shows that 7 lumps should be used for L1 and L2, approximately 30 percent more variables than the procedure developed in this work requires.

Example Two: Shafts have different geometrical parameters.

In this example a 2-segment cascade is considered. The shafts have the same stiffness and elastic modulus but have a difference in the geometrical parameters. The second shaft is twice the length of the first.

Table 3.4 Parameters for Example 2

	Elastic Modulus	Density	Length	Area	k_s	m_s
segment 1	100	100	1.0	0.01	1.0	1.0
segment 2	100	100	2.0	0.01	0.5	2.0

	k_d	m_d	k_d/k_s	m_s/m_d
segment 1	2.46	10.0	2.46	0.1
segment 2	1.23	2.0	2.46	1.0

Apply Modelling Procedure:

1. Say that one wants the first 6 eigenvalues each with less than 10 percent error.

2. Reduce the acceptable error by 1 percent to account for coupling effects. Y'=10-1=9.

3. Distribute the eigenvalues among the segments.

$$\Delta_1=(\pi/2h_1)\sqrt{E_1/\rho_1}=(\pi/2)\sqrt{100/100}=\pi/2 \qquad \Delta_2=\pi/4$$

$$N_2=(\Delta_1/\Delta_2)N_1=2N_1$$

$$X=N_1+N_2$$

$$6=N_1+2N_1 \rightarrow N_1=2 \quad N_2=4$$

4. Since $N_1=2$ and $N_2=4$, the one-segment tables for the first two eigenvalues are used for segment 1 and the tables for the first four

eigenvalues are used for segment 2. Looking in appropriate error tables gives L1=3, L2=8. Assembling the finite dimensional model for the system results in the configuration shown in Figure 3.3. Simulation yields the results shown in Table 3.5 below.

Table 3.5 Eigenvalue Data for Example 2

Eigenvalue	L1=3 L2=8	Evaluation Model	Percent Error
1	0.2122	0.2135	-0.61
2	0.4580	0.4617	-0.80
3	1.2898	1.3107	-1.59
4	2.2237	2.3923	-7.05
5	2.4649	2.6167	-5.80
6	3.7229	4.0940	-9.06

Again the procedure has resulted in a low order model that meets the given model quality index. In contrast to the last example, note here that the number of lumps used for the two continuum elements is similar to what one would use if basing the decision on the continuum elements alone.

Example Three: Shafts have different geometrical and constitutive parameters.

This is another 2-segment example. But here the shafts have different densities in addition to having different lengths.

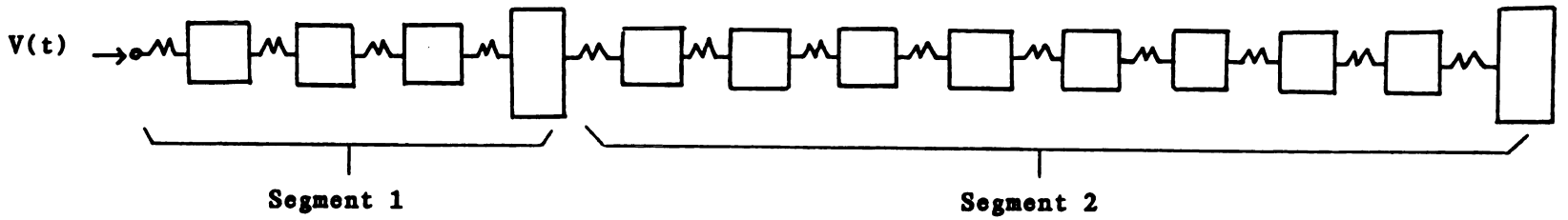

Figure 3.3 Low-Order Model for Example 2

Table 3.6 Parameters for Example 3

	Elastic Modulus	Density	Length	Area	k_s	m_s
segment 1	100	100	1.0	0.01	1.0	1.0
segment 2	100	25	2.0	0.01	0.5	0.5

	k_d	m_d	k_d/k_s	m_s/m_d
segment 1	2.46	10.0	2.46	0.1
segment 2	1.23	0.5	2.46	1.0

Applying Modelling Procedure:

1. Assume that it is desired to have the first six eigenvalues with less than 10 percent error in each.

2. Minus 1 percent for coupling effects. Y'=10-1=9.

3. Distribute the eigenvalues among the segments.

$$\Delta_1=\pi/2 \qquad \Delta_2=\pi/2 \qquad \rightarrow \qquad N_1=N_2$$

$$X=N_1+N_2$$

$$6=2N_1 \qquad \rightarrow \qquad N_1=3 \qquad N_2=3$$

4. $N_1=N_2=3$, so use the tables for the first three eigenvalues for both segments. Looking in the 1-segment error tables with the mass and stiffness ratios from Table 3.6 above gives L1=6, L2=6. Assembling the low-order model and simulating gives the results shown in Table 3.7 below.

Table 3.7 Eigenvalue Data for Example 3

Eigenvalue	L1=6 L2=6	Evaluation Model	Percent Error
1	0.2507	0.2513	-0.24
2	0.7924	0.8073	-1.87
3	2.3113	2.3921	-3.38
4	2.5275	2.5810	-2.07
5	4.7251	5.1658	-8.52
6	4.7805	5.2072	-8.19

Example Four: A General Cascade.

As a final example in illustrating the use of the modelling procedure, consider the four-segment cascade of Figure 3.4 having the parameters given in Table 3.8.

Applying Modelling Procedure:

1. Assume that one wants first 8 eigenvalues each with less than 12 percent error.
2. Minus 1 percent for coupling effects. Y'=12-1=11.
3. Distribute the eigenvalues.

$$\Delta_1=\pi/4 \qquad \Delta_2=5\pi \qquad \Delta_3=\pi/6 \qquad \Delta_4=\pi/2$$

$$N_1=(\Delta_2/\Delta_1)N_2=20N_2 \qquad N_3=(\Delta_2/\Delta_3)N_2=30N_2 \qquad N_4=(\Delta_2/\Delta_4)N_2=10N_2$$

$$X=N_1+N_2+N_3+N_4$$

$$8=61N_2 \rightarrow N_2=.13 \rightarrow N_1=2.6 \quad N_3=3.9 \quad N_4=1.3$$

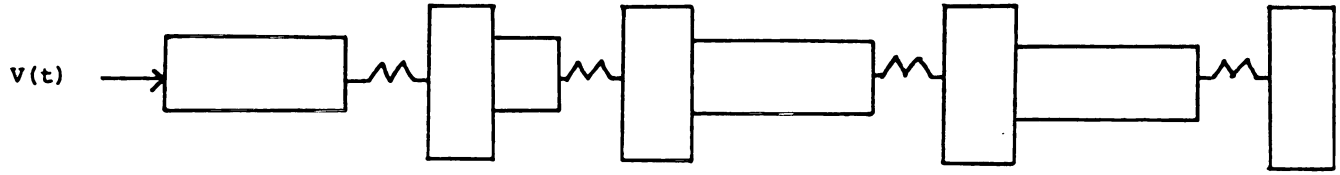

Figure 3.4 Form of Cascade System for Example 4

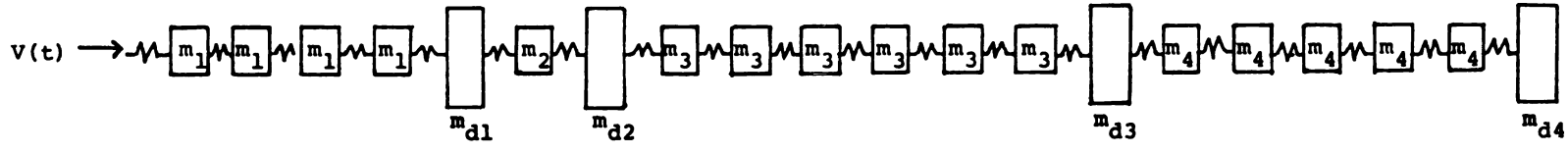

Figure 3.5 Low-Order Model for Example 4

4. So after rounding up, use N_1=3, N_2=1, N_3=4, N_4=2. Looking in the 1-segment error tables under the appropriate eigenvalues with the mass and stiffness ratios from Table 3.8 above gives L1=4, L2=1, L3=6, L4=5. Assembling the low-order model shown in Figure 3.5 and simulating yields the results shown in Table 3.9 below.

Table 3.8 Parameters for Example 4

	segment 1	segment 2	segment 3	segment 4
Elastic Modulus	100	400	50	100
Density	100	4.0	50	25
length	2.0	1.0	3.0	2.0
Area	0.01	0.01	0.01	0.01
k_s	0.5	4.0	0.17	0.5
m_s	2.0	0.04	1.5	0.5
k_d	5.0	2.46	1.65	44.41
m_d	2.0	0.4	1.5	0.05
k_d/k_s	10.0	0.62	9.87	22.21
m_s/m_d	1.0	0.1	1.0	10.0

Table 3.9 Eigenvalue Data for Example 4

Eigenvalue	L1=4, L2=1 L3=6, L4=5	Evaluation Model	Percent Error
1	0.1845	0.1896	-2.69
2	0.4383	0.4470	-1.95
3	0.9628	0.9776	-1.51
4	1.451	1.507	-3.68
5	1.529	1.611	-5.09
6	1.769	1.796	-1.45
7	2.332	2.343	-0.46
8	2.710	2.980	-9.04

Examining the results shows that the modelling procedure yields good results for the general case.

3.3 Behavior of the Eigenvectors

One other issue that bears mentioning here is the "correctness" of the eigenvectors associated with the low-order models generated from the modelling procedure. The modelling procedure is not dependent on the order in which the 1-segments are coupled, so a question naturally arises as to the "correctness" of the eigenvectors.

To examine this question, a 3-segment cascade was considered, with two of the segments being identical and the third segment being different. Let the identical segments be called 'A' segments, and the different segment be called a 'B' segment. Three systems were examined, an AAB, an ABA, and a BAA configuration. Low order models and evaluation models were developed for each configuration. -

Eigenvectors were then examined to determine the "correctness" of the low-order models' eigenvectors.

Examining Figures 3.6, 3.7, and 3.8, which are overlays of each systems' low-order and evaluation model eigenvectors, it is clear that the low-order models give good approximations to the eigenvectors of their corresponding evaluation model. So the modelling procedure, even though it does not account for how the cascade segments are ordered, and has a model quality index based on eigenvalue information only, yields useful information about the system eigenvectors.

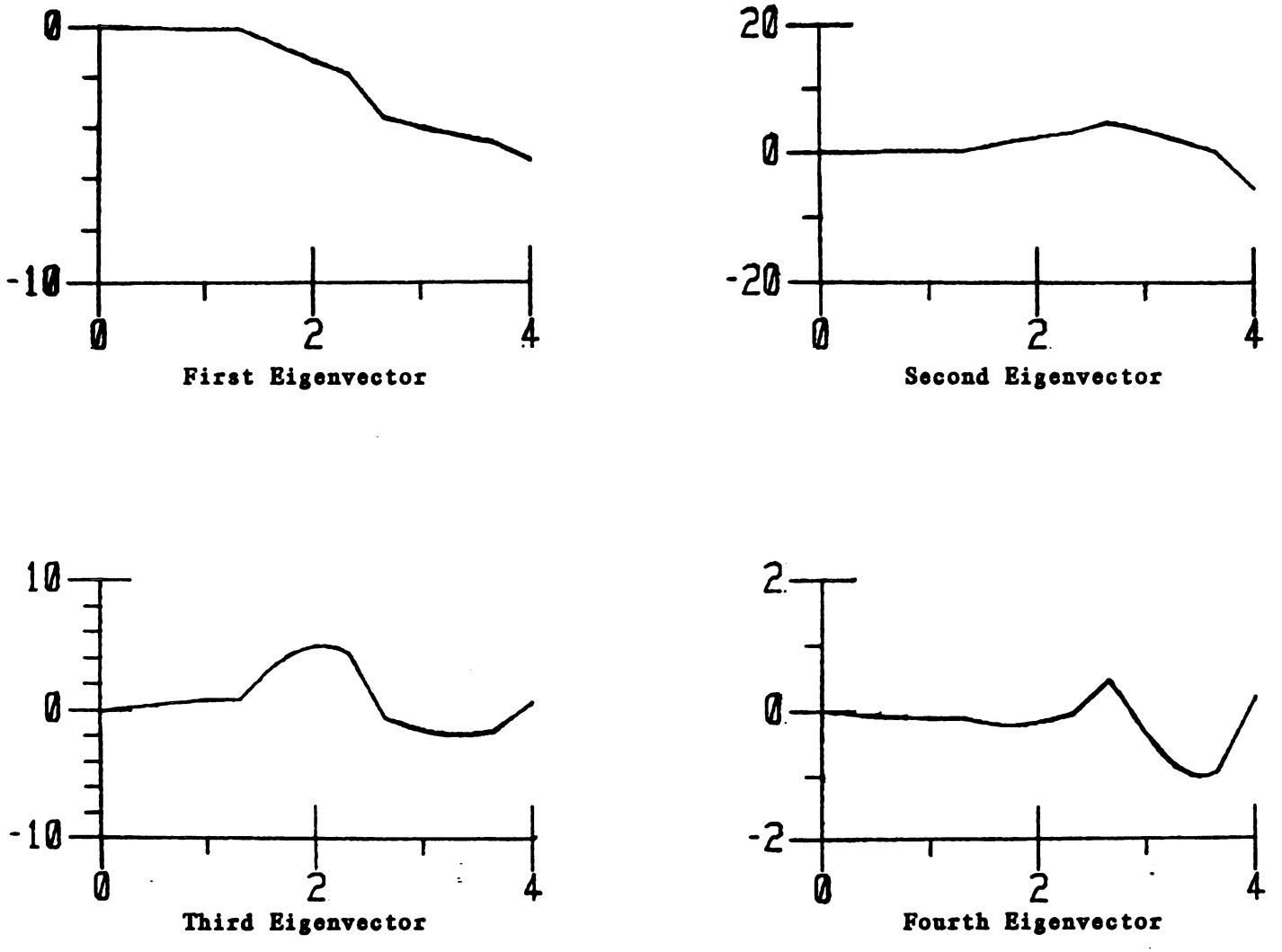

Figure 3.6 Overlay of Low-Order and Evaluation Model Eigenvectors for the BAA Model

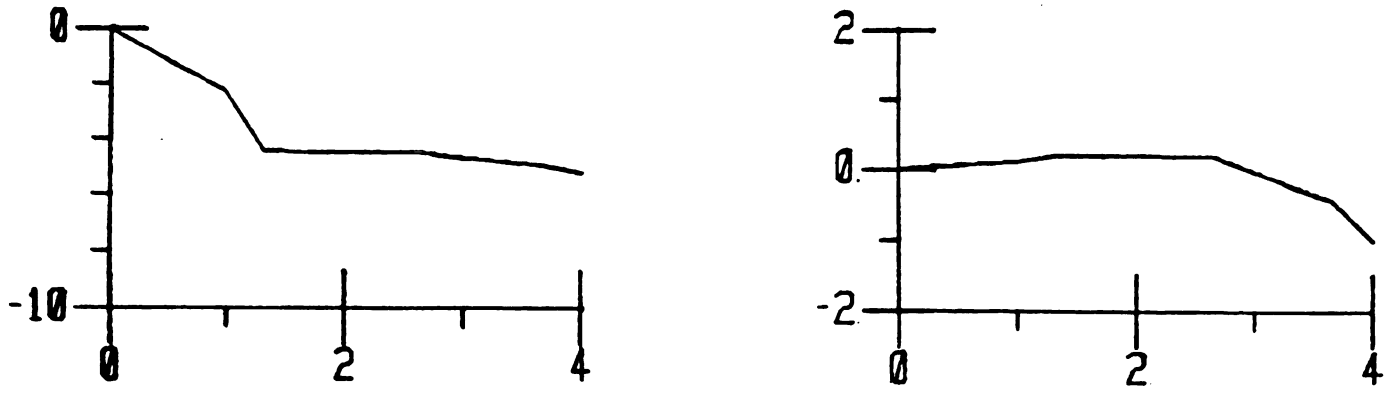

First Eigenvector

Second Eigenvector

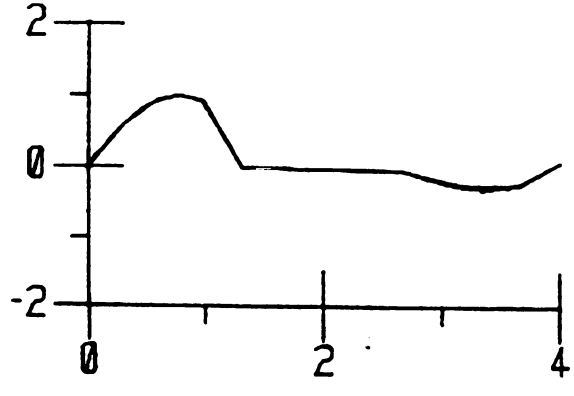

Third Eigenvector

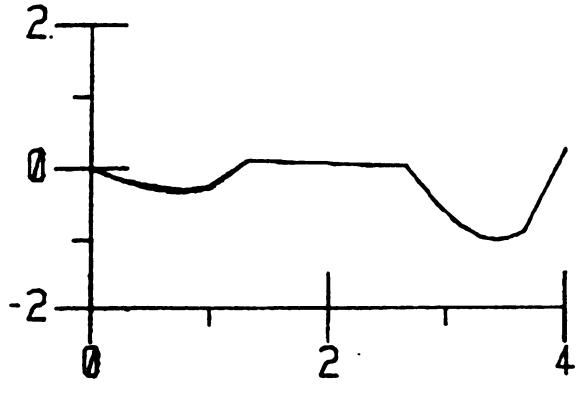

Fourth Eigenvector

Figure 3.7 Overlay of Low-Order and Evaluation Model Eigenvectors for the ABA Model

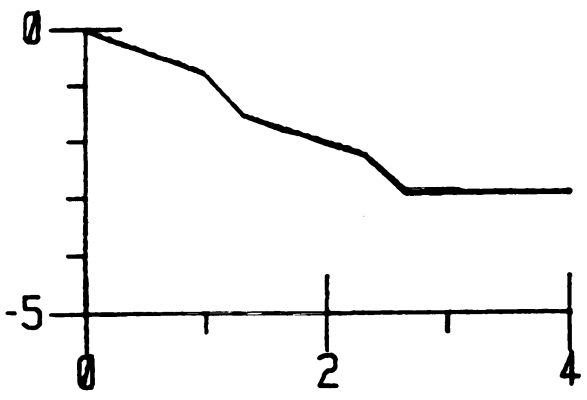

First Eigenvector

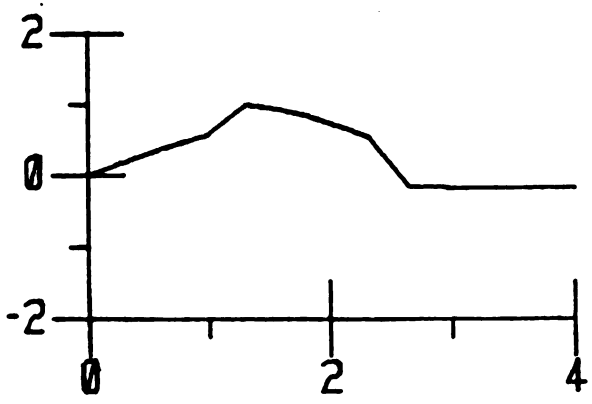

Second Eigenvector

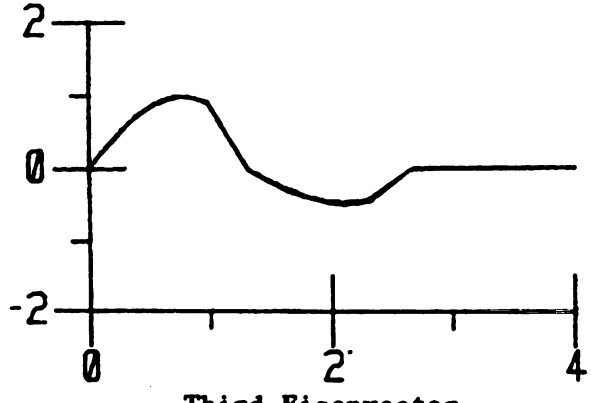

Third Eigenvector

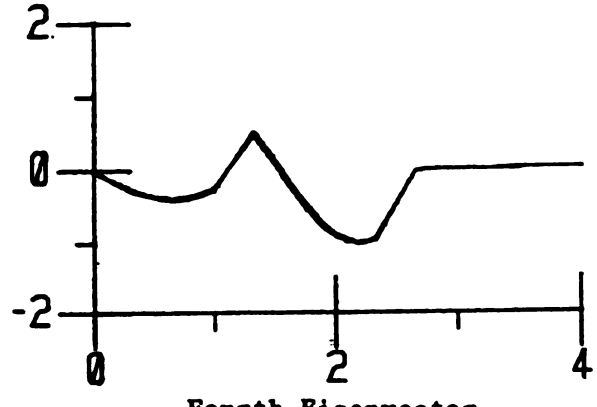

Fourth Eigenvector

Figure 3.8 Overlay of Low-Order and Evaluation Model Eigenvectors for the AAB Model

4. MORE GENERAL CASCADE SYSTEMS

4.1 Relaxation of Restrictions

In this section, some restrictions of Chapter 1 will be relaxed. Some examples will be considered to demonstrate the usefulness of the modelling procedure in situations where the restrictions of Chapter 1 are not met. The particular restriction to be relaxed is that the discrete subsystems must be of the form shown in Figure 1.4. Now the discrete subsystems will be permitted to have any one of the following forms:

1. spring-mass
2. mass-spring
3. mass-spring-mass
4. spring-mass-spring
5. spring-mass-spring-mass

The first of these forms (spring-mass) is the form of the discrete subsystem used in developing the modelling procedure and is shown in Figure 1.4. The other permissible forms of the discrete subsystem are shown in Figures 4.1, 4.2, 4.3, and 4.4.

The modelling procedure given in Chapter 3 requires that a stiffness ratio and a mass ratio be defined for each segment. For the discrete subsystem forms shown in Figures 4.2, 4.3, and 4.4, it is possible to define more than one mass ratio or more than one stiffness ratio for a segment. To use the modelling procedure unambiguously, only a single mass and a single stiffness can be associated with each discrete subsystem. To do this, a "first-oscillator-in" concept was used. This notion is that for a segment, the discrete spring and

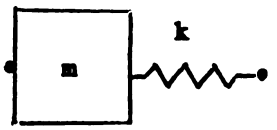

Figure 4.1 Mass-Spring Subsystem

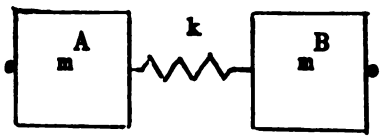

Figure 4.2 Mass-Spring-Mass Subsystem

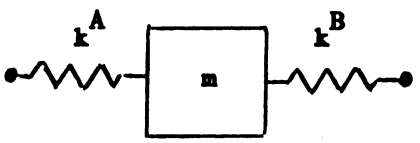

Figure 4.3 Spring-Mass-Spring Subsystem

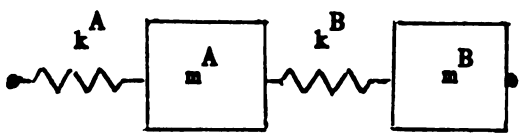

Figure 4.4 Spring-Mass-Spring-Mass Subsystem

discrete mass nearest to the continuum element have a much greater effect than the other springs and masses in the discrete subsystem. Consider the segment shown in Figure 4.5. Using the "first-oscillator-in" notion, the mass ratio and the stiffness ratio to use with the modelling procedure are m_s/m_d^A and k_d^A/k_s.

Using the "first-oscillator-in" concept, the modelling procedure can be applied directly to systems having discrete subsystems with more than one spring or more than one mass element. The following examples demonstrate the usefulness of the modelling procedure for cascade systems with more general discrete subsystems such as those shown in Figures 4.1 through 4.4.

Example Five: Two segment cascade with a mass-spring discrete subsystem.

Consider the system shown in Figure 4.6 with the parameters given in Table 4.1 below. This example is the same as example two except that the discrete subsystem in the first segment is reversed.

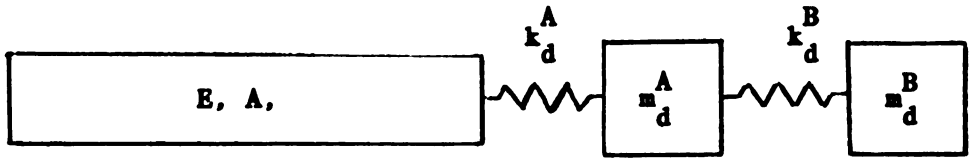

Figure 4.5 First-Oscillator-In Illustration

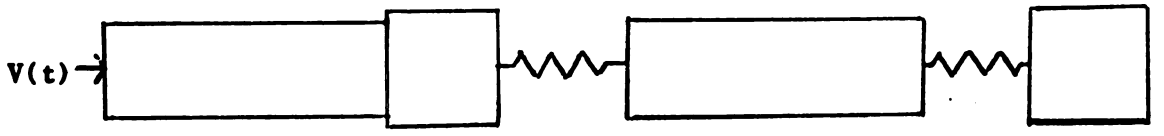

Figure 4.6 System of Example 5

Table 4.1 Parameters for Example 5

	Elastic Modulus	Density	Length	Area	k_s	m_s
segment 1	100	100	1.0	.01	1.0	1.0
segment 2	100	100	2.0	.01	0.5	2.0

	k_d	m_d	k_d/k_s	m_s/m_d
segment 1	1.0	1.0	1.0	1.0
segment 2	1.0	1.0	1.0	1.0

Applying Modelling Procedure:

1. Say that one wants first 6 eigenvalues each with less than 10 percent error.

Application of the modelling procedure follows exactly as in example two. To meet the model quality index one should use L1=3 and L2=8. Assembling the low-order model and simulating gives the results shown in Table 4.2 below.

Table 4.2 Eigenvalue Data for Example 5

Eigenvalue	L1=3 L2=8	Evaluation Model	Percent Error
1	0.2377	0.2399	-0.92
2	0.4405	0.4450	-1.01
3	1.150	1.155	-0.43
4	2.212	2.271	-2.60
5	3.024	3.173	-4.70
6	3.449	3.621	-4.75

The results meet the specified model quality index, so the procedure is seen to be useful for a cascade having this type of discrete subsystem.

Example Six: Two-segment cascade having a mass-spring-mass discrete subsystem.

Consider the system shown in Figure 4.7 with the parameters given in Table 4.3 below.

Table 4.3 Parameters for Example 5

	Elastic Modulus	Density	Length	Area	k_s	m_s
segment 1	100	25	1.0	.01	1.0	.25
segment 2	100	25	1.0	.01	1.0	.25

	k_d	m_d^A	k_d/k_s	m_s/m_d^A	m_d^B
segment 1	.6169	2.5	.6169	0.1	.25
segment 2	.6169	.25	.6169	1.0	

Applying Modelling Procedure:

1. Say that one wants first 4 eigenvalues each with less than 12 percent error.

2. Minus 1 percent for coupling effects. Y'=12-1=11.

3. Distributing the eigenvalues:

$$\Delta_1=\pi \qquad \Delta_2=\pi \rightarrow N_1=N_2$$

$$X=N_1+N_2$$

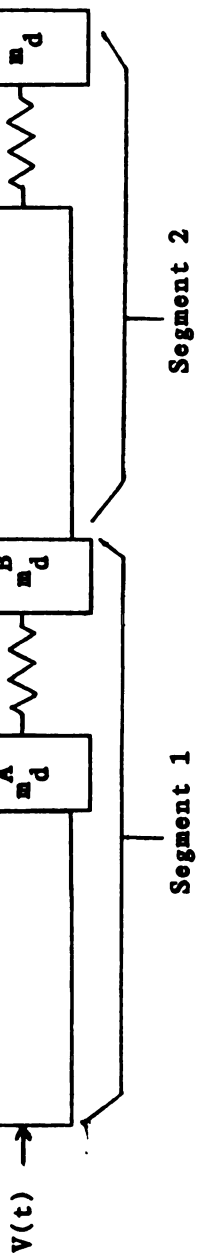

Figure 4.7 System of Example 6

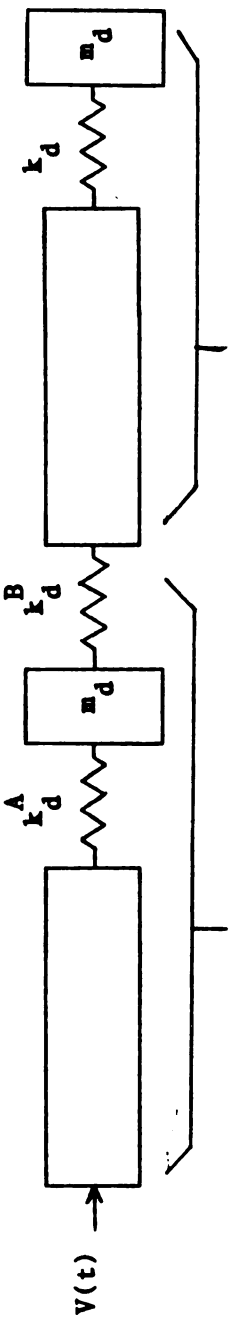

Figure 4.8 System of Example 7

$4=2N_2$ $N_1=2$ $N_2=2$

4. $N_1=N_2=2$, so use the tables for the first two eigenvalues for both segments. Looking in the appropriate 1-segment error tables with the mass and stiffness ratios from the parameter table above gives L1=4, L2=3. Assembling the low-order model and simulating yields the results below.

Table 4.4 Eigenvalue Data for Example 6

Eigenvalue	L1=4 L2=3	Evaluation Model	Percent Error
1	0.5062	0.5093	-0.61
2	0.9321	0.9442	-1.28
3	1.916	1.869	2.51
4	4.188	4.634	-9.62

The errors are all within the 12 percent allowed by the specified model quality index, so the procedure is seen to be useful for a cascade system with a mass-spring-mass subsystem.

Example Seven: Two-segment cascade with a spring-mass-spring discrete subsystem.

Consider the system shown in Figure 4.8 with the parameters given in Table 4.5 below.

Table 4.5 Parameters for Example 7

	Elastic Modulus	Density	Length	Area	k_s	m_s
segment 1	1.0	1.0	1.0	1.0	1.0	1.0
segment 2	1.0	1.0	1.0	1.0	1.0	1.0

	k_d^A	m_d^A	k_d^A/k_s	m_s/m_d^A	k_d^B
segment 1	1.0	1.0	1.0	1.0	1.0
segment 2	1.0	1.0	1.0	1.0	

Applying Modelling Procedure:

1. Say that one wants first 4 eigenvalues each with less than 10 percent error.

2. Minus 1 percent for coupling effects. Y'=10-1=9.

3. Distributing the eigenvalues:

$$\Delta_1=\pi/2 \qquad \Delta_2=\pi/2 \rightarrow N_1=N_2$$

$$X=N_1+N_2$$

$$4=2N_2 \qquad N_1=2 \qquad N_2=2$$

4. $N_1=N_2=2$, so use the tables for the first two eigenvalues for both segments. Looking in the appropriate 1-segment error tables with the mass and stiffness ratios from the parameter table above gives L1=3, L2=3. Assembling the low-order model and simulating yields the results below.

Table 4.6 Eigenvalue Data for Example 7

Eigenvalue	L1=3 L2=3	Evaluation Model	Percent Error
1	0.3280	0.3328	-1.42
2	0.9285	0.9377	-0.97
3	1.5685	1.596	-1.72
4	1.9713	2.143	-8.01

The results satisfy the specified model quality index, so the procedure gives useful results for a cascade having a spring-mass-spring discrete subsystem.

Example Eight: Cascade with discrete subsystems having two degrees-of-freedom in a spring-mass-spring-mass configuration. Now consider the system of Figure 4.9 with the parameters given in Table 4.7 below.

Table 4.7 Parameters for Example 8

	Elastic Modulus	Density	Length	Area	k_s	m_s
segment 1	1.0	1.0	1.0	1.0	1.0	1.0
segment 2	1.0	1.0	1.0	1.0	1.0	1.0

	k_d^A	m_d^A	k_d^A/k_s	m_s/m_d^A	k_d^B	m_d^B
segment 1	1.0	1.0	1.0	1.0	1.0	1.0
segment 2	1.0	1.0	1.0	1.0	1.0	1.0

Applying Modelling Procedure:

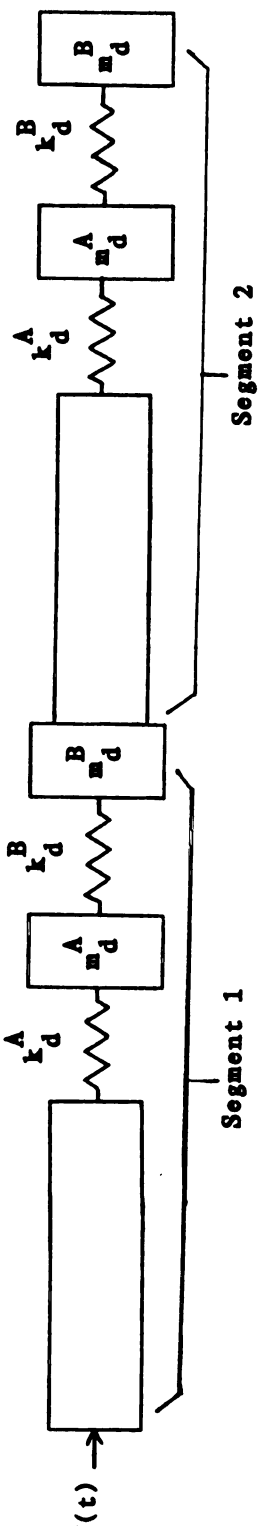

Figure 4.9 System of Example 8

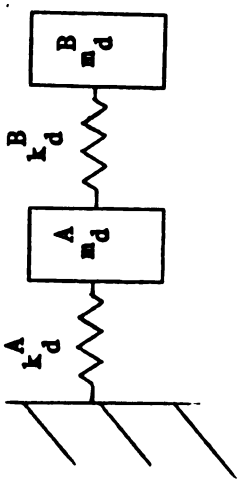

Figure 4.10 Discrete Subsystem from Example 8

1. Assume that it is desired to have the first 8 eigenvalues each with less than 15 percent error.

2. Subtract 1 percent for coupling effects. Y'=15-1=14.

3. Distributing the eigenvalues:

$$\Delta_1=\pi/2 \qquad \Delta_2=\pi/2 \qquad N_1=N_2$$

$$X=N_1+N_2$$

$$8=2N_2 \quad \rightarrow \quad N_2=4 \qquad N_1=4$$

4. $N_1=N_2=4$, so use the tables for the first four eigenvalues for both segments. Looking in the 1-segment error tables with the mass and stiffness ratios from Table 4.7 above gives L1=6, L2=6. Simulation gives the results shown in Table 4.8 below.

Table 4.8 Eigenvalue Data for Example 8

Eigenvalue	L1=6 L2=6	Evaluation Model	Percent Error
1	0.2459	0.2468	-0.34
2	0.7056	0.7019	0.53
3	1.271	1.292	-1.61
4	1.567	1.566	0.09
5	2.057	2.144	-4.05
6	2.409	2.498	-3.54
7	4.458	4.921	-9.39
8	4.641	5.11	-9.17

The errors here are all well under the 15 percent allowed by the choice of model quality index. So for cascade linear mixed-structure systems where the discrete subsystems have a spring-mass-spring-mass structure, the modelling procedure is still useful.

This example also serves to illustrate an interesting artifact that occurs when identical segments are coupled together as they are in example six. Note that some of the eigenvalues in the low-order model have positive errors. In this example, the second and fourth eigenvalues have positive errors. The interesting thing to note about these eigenvalues is that their frequencies correspond closely with those of the discrete subsystem. Consider the discrete subsystem shown in Figure 4.10. The equations of motion for this system are:

$$\begin{bmatrix} 1 & 0 \\ 0 & 1 \end{bmatrix} \ddot{x} + \begin{bmatrix} 2 & -1 \\ -1 & 1 \end{bmatrix} x = 0$$

Solving the system equations for the eigenvalues gives $\omega = \{0.62, 1.62\}$. Comparing with the true spectrum for the linear system of example 6 shows that these eigenvalues correspond closely with the second (0.7056) and the fourth (1.5663) eigenvalues.

In examples five through eight above, it has been shown that the modelling procedure is useful for cascades more general than those that were used in developing the procedure. As a final illustration of the usefulness of the procedure in general cascade systems, consider example nine below.

Example Nine: Cascade with a force input.

The system in this example is identical to that in example two (shown in Figure 3.1) with the exception that the velocity input in example two is replaced with a force input here. Suppose that as in example two, the model quality index is that the first six eigenvalues each have less than 10 percent error. The modelling procedure does not account for the type of input, so following through example two, one finds that for the low-order model, L1=3 and L2=8. Assembling the low-order model shown in Figure 4.11 and simulating yields the results shown in Table 4.9 below.

Table 4.9 Eigenvalue Data for Example 9

Eigenvalue	L1=3 L2=8	Evaluation Model	Percent Error
1	0.0000	0.0000	0.00
2	0.4319	0.4361	-0.96
3	1.262	1.179	7.04
4	1.343	1.319	1.82
5	2.462	2.615	-5.85
6	3.628	3.732	-2.79
7	3.723	4.094	-9.06

Even if the zero eigenvalue is assumed given, the results still meet the model quality index. So the procedure is seen to be useful for a cascade having a force input.

It is interesting to note here the type of physical lumping used for the continuum element in segment one. As in all other discretizations in this work, a spring-mass physical lumping was used.

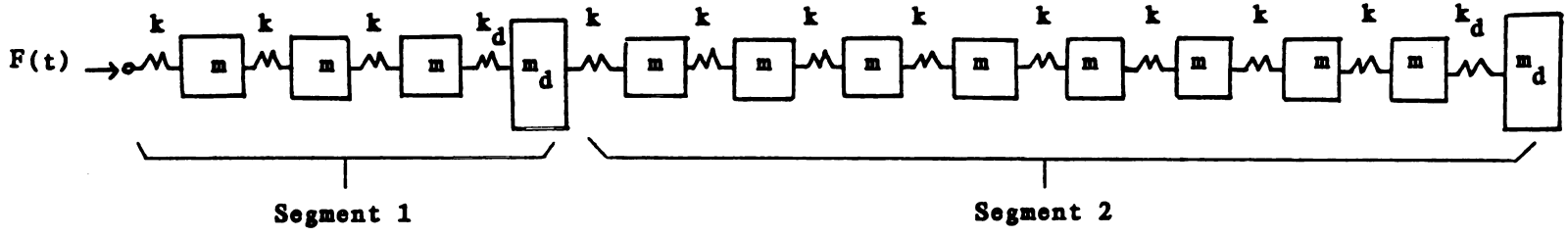

Figure 4.11 Low-Order Model for Example 9

But in segment one, the spring element next to the force input is dependent. Since the continuum element is causally independent, one might consider it "better" to use a physical lumping discretization that has mass elements at both ends, such as the discretization shown in Figure 4.12. But comparing the errors in example nine with those from example two, where the discretization matches the end conditions, shows that they are quite similar although the correspondence in not one-to-one. The effect on the errors of choosing the type of physical lumping based on the shaft's end conditions is an area that has not been adequately explored yet.

4.2 Modifying the Procedure under Certain Conditions

One last thing to be discussed is a caution concerning the use of the modelling procedure. In modelling cascades where there are two identical segments coupled together and also segments having higher frequency spectra than the identical ones, if one is interested in relatively few eigenvalues, then step 3 in the procedure should be modified slightly. Before discussing this modification, the difficulty is illustrated in the following example.

Consider an AAB configuration of a 3-segment cascade where the 'A' and 'B' segments have the parameters given below.

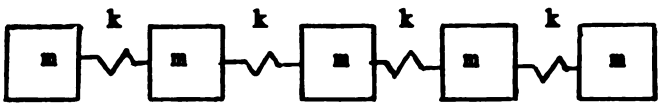

Figure 4.12 Physical Lumping Discretization Having Mass Elements at Both Ends

Table 4.10 Parameters for AAB Example

	Elastic Modulus	Density	Length	Area	k_s	m_s
A segments	1.0	1.0	1.0	1.0	1.0	1.0
B segment	20.0	5.0	1.0	1.0	20.0	5.0

	k_d	m_d	k_d/k_s	m_s/m_d
A segments	1.0	1.0	1.0	1.0
B segment	200.0	0.5	10.0	10.0

Assume that one wants the first 5 eigenvalues with less than 10 percent error in each. Following through the modelling procedure gives N_A=2, N_B=1. Checking the 1-segment tables gives LA=4, LB=5. Assembling the low-order model and simulating yields the eigenvalues below.

Table 4.11 Eigenvalue Data for AAB Example

Eigenvalue	LA=4 LB=5	Evaluation Model	Percent Error
1	0.1853	0.1859	-0.32
2	0.7996	0.7916	1.01
3	1.860	2.029	-8.33
4	2.308	2.457	-6.06
5	4.174	4.896	-14.75

Examining the results shows that the fifth eigenvalue has too-large an error. To explain this, examine the evaluation model eigenvalues for the 'A' segment, the 'B' segment, and the 2-segment AA component given

in Table 4.12.

Table 4.12 Evaluation Model Eigenvalues for Components of AAB Cascade

Eigenvalue	'A' segment	'B' segment	'AA' component
1	0.6762	2.85	0.3667
2	2.117	8.47	1.005
3	4.921	13.85	2.042
4	7.98	19.04	2.495
5	11.086	24.3	4.91

Comparing the eigenvalues with those from the AAB evaluation model reveals the difficulty. The procedure indicated that one of the five eigenvalues should come from the 'B' segment (N_B=1). But comparing the eigenvalues shows that all five came from the 2-segment 'AA' component. The solution to this problem is to modify step 3 in the procedure to:

1. Round the N values up to the nearest integer.

2. For the identical coupled segments, increase their N value by one.

Re-examining the problem using the modified procedure gives N_A=3, N_B=1, and from the error tables one gets that LA=7, LB=5. Assembling the model and simulating gives the results below.

Table 4.13 Eigenvalue Data for AAB Example using Modified Procedure

Eigenvalue	LA=7 LB=5	Percent Error
1	0.1855	-0.22
2	0.7962	0.58
3	1.932	-4.78
4	2.374	-3.38
5	4.521	-7.65

So the modification to the procedure corrected the difficulty. A note on this is that the difficulty does not arise if one is interested in a relatively large number of eigenvalues. Consider the same problem but now assume that one wants the first 10 eigenvalues with less than 10 percent error in each. Using the unmodified procedure gives N_A=4, N_B=2, and LA=9, LB=5. Simulating yields the following results, which do meet the model quality index requirement.

Table 4.14 Eigenvalue Data for AAB Example with Model Quality Index Based on the First Ten Eigenvalues

Eigenvalue	LA=9 LB=5	Evaluation Model	Percent Error
1	0.1856	0.1859	-0.16
2	0.7951	0.7916	0.44
3	1.9539	2.0299	-3.74
4	2.3935	2.4570	-2.58
5	4.6172	4.896	-5.69
6	4.755	4.901	-2.96
7	4.900	5.133	-4.53
8	7.343	7.999	-8.19
9	7.457	8.126	-8.22
10	9.438	9.872	-4.39

APPENDICES

5. SUMMARY AND CONCLUSIONS

The most important result of this work is the development of a modelling procedure to directly generate efficient low-order models for cascade linear mixed-structure systems. The procedure is a five-step method in which the designer specifies a model quality index, uncouples the cascade, distributes the eigenvalues of interest among the segments, discretizes the segments individually using the error tables, and then assembles the low-order model. Developed using some restrictive assumptions, this modelling procedure was shown in Chapter 4 to still be useful when the assumption concerning the form of the discrete subsystems is violated. This procedure gives the systems modeller a rational approach to modelling linear mixed-structure systems, helping to remove the modelling of these types of systems from the realm of a "black art".

In Chapter 2, two interesting techniques for generating the eigenvalues of linear mixed-structure systems are introduced. The first of these generates analytical solutions for linear mixed-structure systems having only one continuum element. In contrast to other solution techniques for these systems [7,8], it requires no a priori knowledge of the continuum element's eigenvalue and eigenvector behavior.

The other technique generates evaluation model eigenvalues using a sequence of relatively low-order discretized representations of the system. It exploits the convergence behavior of the discretizing technique in an absolute sense by applying a least squares technique to a truncated convergence rate expression, in order to generate the

evaluation model eigenvalues. While applied here to linear mixed-structure systems discretized using a physical lumping approach, its usefulness does not appear to be limited to these cases.

Future efforts in modelling linear mixed-structure systems would most naturally be directed toward examining application of the modelling procedure to other types of system topologies and development of an analogous modelling procedure based on finite element discretizations. With further development of the 1-segment error tables, it may be useful to implement the modelling procedure within modelling and simulation programs such as ENPORT-5 [10] and MEDUSA [11].

One final note is that since the procedure is only a guideline and connot guarantee that the results will meet the model quality index, it may be desireable in some cases to increase one's confidence in the results. One possible way to do this is to follow through the procedure to find the number of lumps to use. But when assembling the low-order model, replace the physical lumping discretizations with a method having a faster convergence rate, such as a linear finite element, using the number of lumps (elements) given by the procedure.

APPENDIX A

SOLUTION TO THE FINITE DIFFERENCE PROBLEM

To solve the System in (A-1),

$$-EAL/h)(\theta_{n+1}-2\theta_n+\theta_{n-1})=\omega^2(\rho Ah/L)\theta_n \qquad (A-1)$$

$$\theta_0=0 \qquad (\theta_{L+1}-\theta_L)/(h/L)=0 \qquad (A-2)$$

first use the central difference operator notation

$$\Delta\ \theta_n=\theta_{n+1}-2\theta_n+\tau_{n-1} \qquad (A-3)$$

to rewrite the system equations (A-1) in the form (A-4).

$$-\Delta\ \theta_n=((\omega^2\rho h^2)/(EL^2))\theta_n \qquad (A-4)$$

Using the finite difference identity (A-5) from Goudreau [12],

$$\Delta \begin{bmatrix} \sin(\lambda n/L) \\ \cos(\lambda n/L) \end{bmatrix}=-4\sin^2(\lambda/2L)\begin{bmatrix} \sin(\lambda n/L) \\ \cos(\lambda n/L) \end{bmatrix} \qquad (A-5)$$

the general solution to the system equation is:

$$\theta_n=A\sin(\lambda n/L)+B\cos(\lambda n/L) \qquad (A-6)$$

The $\theta_0=0$ boundary condition gives B=0. Applying the other boundary condition:

$$(\theta_{L+1}-\theta_L)/(h/L)=0 \qquad \text{(A-2)}$$

$$\sin(\lambda(L+1)/h)-\sin\lambda=0 \qquad \text{(A-7)}$$

Applying a trigonometric identity to equation (A-7) gives:

$$\cos(0.5\lambda(2L+1)/L)\sin(0.5\lambda(1/L))=0 \qquad \text{(A-8)}$$

So either:

$$\lambda=2j\pi L \qquad j=1,2,3,. \ . \ . \qquad \text{(A-9)}$$

or

$$\lambda=(L/(2L+1))(2j-1)\pi \qquad j=1,2,3,. \ . \ . \qquad \text{(A-10)}$$

Substituting (A-9) into the general solution (A-6) gives

$$\theta_n=A\sin(2j\pi n)=0 \qquad \text{(A-11)}$$

So $\lambda=2j\pi L$ results in the trivial solution. Substituting (A-10) into the general solution yields:

$$\theta_n=A\sin[(2j-1)\pi n/(2L+1)] \qquad n=1,2,. \ . \ .,L \quad j=1,2,. \ . \ . \qquad \text{(A-12)}$$

So the displacements at the points n=1,2,. . .,L are determined by a set of sine functions. Comparing equations (A-4) and (A-5) results in

the following expression for the natural frequencies.

$$4\sin^2[\lambda/2L]=\omega^2\rho h^2/EL^2 \qquad \text{(A-13)}$$

Using equation (A-10) to substitute for λ and solving (A-13) for ω gives:

$$\omega_j=(2L/h)\ E/\rho\ \sin[(2j-1)\pi/(4L+2)] \quad j=1,2,\ .\ .\ .,L \qquad \text{(A-14)}$$

Dividing by the solution (A-15) to the continuum boundary value problem and subtracting 1 gives the error expression shown in section 2.2 and reproduced below in (A-16).

$$\bar{\omega}_j=((2j-1)\pi/2)\sqrt{E/\rho} \qquad \text{(A-15)}$$

$$[(\omega-\bar{\omega})/\bar{\omega}]=(4L/(2j-1)\pi)\sin[(2j-1)\pi/(4L+2)]-1 \quad j=1,2,\ .\ .\ .\ ,L \qquad \text{(A-16)}$$

APPENDIX B

DIRECT SOLUTION TO THE BOUNDARY VALUE PROBLEM FOR THE PROTOTYPE LINEAR MIXED-STRUCTURE SYSTEM.

For the prototype linear mixed-structure system of Figure 3.1a, the boundary value problem is:

$$\partial^2 u/\partial x^2 = 1/a^2 \partial^2 u/\partial t^2 \qquad a^2 = E/\rho \tag{B-1}$$

$$m_d \ddot{y}(t) = -k_d(y(t) - u(h,t)) \tag{B-2}$$

$$u(0,t) = 0 \qquad EA(\partial u/\partial x)_{x=h} = k_d(y(t) - u(h,t)) \tag{B-3}$$

Assume that $y(t) = cu(h,t)$. (B-4)

Substituting into (B-2) and (B-3) gives

$$m_d c \partial^2 u(h,t)/\partial t^2 = -k_d u(h,t)(c-1) \tag{B-5}$$

$$EA(\partial u/\partial x)_{x=h} = k_d u(h,t)(c-1) \tag{B-6}$$

Applying the standard separation of variables assumption

$$u(x,t) = P(x)Q(t) \tag{B-7}$$

to the boundary value problem gives:

$$a^2P''(x)/P(x)=Q''(t)/Q(t)=-\omega^2 \tag{B-8}$$

$$P(0)=0 \tag{B-9}$$

$$EAP'(h)=k_dP(h)(c-1) \tag{B-10}$$

From equation (B-8), one obtains:

$$Q''(t)+\omega^2Q(t)=0 \tag{B-11}$$

$$P''(x)+(\omega/a)^2P(x)=0 \tag{B-12}$$

The solution to equation (B-12) is

$$P(x)=D\sin(\omega x/a)+F\cos(\omega x/a) \tag{B-13}$$

Using the boundary condition in (B-9) gives F=0. So

$$P(x)=D\sin(\omega x/a) \tag{B-14}$$

Substituting equation (B-14) into (B-10) gives

$$(\omega/a)\cos(\omega h/a)=k_d(c-1)/EA)\sin(\omega h/a) \tag{B-15}$$

$$\omega=(ak_d/EA)(c-1)\tan(\omega h/a) \tag{B-16}$$

This equation represents the frequency relation for the shaft.

Applying the same separation of variables to equation (B-5) yields

$$m_d c P(h) Q''(t) + k_d (c-1) P(h) Q(t) = 0 \qquad \text{(B-17)}$$

$$Q''(t) + (k_d (c-1)/m_d c) Q(t) = 0 \qquad \text{(B-18)}$$

So the natural frequency of the discrete portion is

$$\omega_d = (k_d (c-1)/m_d c)^{1/2} \qquad \text{(B-19)}$$

At a system natural frequency, $\omega_d = \omega$. So Solving (B-19) for c and substituting into equation (B-16) results in the following frequency relation for the system.

$$\omega = (a k_d / EA)(\omega^2 m_d / (k_d - \omega^2 m_d)) \tan(\omega h / a) \qquad \text{(B-20)}$$

APPENDIX C

THE ONE-SEGMENT ERROR TABLES

The results in the following tables are for one-segment cascade systems as shown in Figure 2.2a, discretized into the form in Figure 2.3. As discussed in section 2.2.2, there are three key parameters in the discretized one-segment system. They are the stiffness ratio k_d/k_s, the mass ratio m_s/m_d, and the number of spring-mass lumps L used to discretize the continuum element.

The error tables are structured as follows. They are first grouped according to the eigenvalue number. That is, there is a set of tables for the first eigenvalue, a set for the second eigenvalue, and so on. For each page in the tables, a mass ratio is specified. Each row on a given table corresponds to a different L value and each column on a given table to a different stiffness ratio. The entries in the tables are the magnitudes of the errors (in percent) in the low order models. The errors are calculated using the relation (C-1).

$$\text{Error} = \left| (\omega - \omega_{true}/\omega_{true})100 \right| \qquad \text{(C-1)}$$

To use the tables, one begins by obtaining the reduced acceptable error Y', the mass ratio m_s/m_d, the stiffness ratio k_d/k_s, and the number of eigenvalues N associated with the given 1-segment. For the segment, the sets of error tables for the first N eigenvalues must be examined. The mass ratio indicates which table in each set to use. The stiffness ratio indicates a particular column in each table.

Beginning with the appropriate table and column for the first eigenvalue, one merely reads down the column until an entry is found that is less than Y'. Reading across the table gives the number of lumps $L^{(1)}$ needed to meet the error criterion for the first eigenvalue. Checking the appropriate table and column for the second through the Nth eigenvalues gives values $L^{(2)}$ through $L^{(N)}$. Choosing the largest of the values $L^{(1)}$ through $L^{(N)}$ gives the number of lumps L to use to discretize the segment.

To illustrate use of the tables, consider example two from Chapter 3. Segment 1 in this example has 2 eigenvalues associated with it, so the sets of tables C.1.1, C.1.2, C.1.3 and C.2.1, C.2.2, C.2.3, corresponding to the first two eigenvalues, will be used. The mass ratio is 0.1. This specifies that tables C.1.1 and C.2.1 are to be used. The stiffness ratio is 2.46 which corresponds to the second column in each table. So one follows down the second column in each table until an entry is reached that has a value less than Y'.(Here Y'=9). Finding this entry and reading across the table shows that for the first eigenvalue, $L^{(1)}=1$, and for the second eigenvalue, $L^{(2)}=3$. Choosing the largest of these requires that 3 spring-mass lumps must be used to discretize segment 1.

Segment 2 has 4 eigenvalues associated with it, so the sets of tables: C.1.1, C.1.2, C.1.3; C.2.1, C.2.2, C.2.3; C.3.1, C.3.2, C.3.3; and C.4.1, C.4.2, C.4.3 will be used. The mass ratio is 1.0 for segment 2, therefore tables C.1.2, C.2.2, C.3.2, and C.4.2 will be used. The stiffness ratio for this segment is 2.46, so one must follow down the second column to find an entry less than Y'. Checking this column shows that the first entry less than Y' occurs when

$L^{(1)}=2$, $L^{(2)}=2$, $L^{(3)}=6$, and $L^{(4)}=8$. So 8 spring-mass lumps will be used to discretize segment 2.

As another illustration of the use of the tables, consider example one from Chapter 3. Three eigenvalues are associated with each segment in the system. So the sets of tables corresponding to the first three eigenvalues will be used. For both segments, the mass ratio is one, so tables C.1.2, C.2.2, and C.3.2 will be used. For segment 1, the stiffness ratio is 16, and for segment 2 it is 1.0. Now just follow down the appropriate columns until the entry is less than the reduced acceptable error Y'. In this problem, both stiffness ratios are between columns on the table. So one must interpolate in some fashion. One could either interpolate linearly, or more conservatively, one could require the entries in both columns to be less than Y'. Choosing the latter option, for segment one, $k_d/k_s=16$, so one would search columns three and four. Following down these two columns, at $L^{(1)}=2$, $L^{(2)}=3$, $L^{(3)}=4$, the entries in both columns are less than Y'=9. Choosing the largest of these values gives L1=4. For segment two, $k_d/k_s=1$, so examine columns one and two. When $L^{(1)}=2$, $L^{(2)}=4$, and $L^{(3)}=7$, the entries in both columns are less than Y'. Again, choosing the largest of these gives L2=7. So in the low-order model, one would use L1=4, L2=7.

Table C.1.1 First Eigenvalue

ms/md=0.1

Number of Lumps	Stiffness Ratio (kd/ks)							
	0.6169	2.4674	9.8696	22.206	39.478	61.685	88.820	120.90
1	0.47	1.66	2.59	2.82	2.96	2.98	3.01	3.03
2	0.21	0.73	1.16	1.27	1.31	1.34	1.35	1.35
3	0.14	0.46	0.74	0.81	0.84	0.86	0.86	0.87
4	0.10	0.34	0.54	0.60	0.61	0.63	0.63	0.63
5	0.08	0.27	0.43	0.47	0.48	0.49	0.50	0.50
6	0.07	0.22	0.35	0.39	0.40	0.41	0.41	0.41
7	0.05	0.19	0.30	0.33	0.34	0.35	0.35	0.35
8	0.05	0.16	0.26	0.29	0.30	0.30	0.30	0.30
9	0.04	0.14	0.23	0.25	0.26	0.27	0.27	0.27
10	0.04	0.13	0.21	0.23	0.23	0.24	0.24	0.24
11	0.03	0.11	0.19	0.21	0.21	0.22	0.22	0.22
12	0.03	0.11	0.17	0.19	0.19	0.20	0.20	0.20
13	0.03	0.09	0.16	0.17	0.18	0.18	0.18	0.18
14	0.03	0.09	0.15	0.16	0.17	0.17	0.17	0.17
15	0.02	0.08	0.14	0.15	0.15	0.16	0.16	0.16
16	0.02	0.08	0.13	0.14	0.14	0.15	0.15	0.15
17	0.02	0.07	0.12	0.13	0.14	0.14	0.14	0.14
18	0.02	0.07	0.11	0.12	0.13	0.13	0.13	0.13

Table C.1.2 First Eigenvalue

ms/md=1.0

Number of Lumps	Stiffness Ratio (kd/ks)							
	0.6169	2.4674	9.8696	22.206	39.478	61.685	88.820	120.90
1	5.57	13.37	16.63	17.27	17.51	17.62	17.67	17.72
2	2.39	6.40	8.39	8.77	8.91	8.98	9.02	9.04
3	1.51	4.17	5.59	5.85	5.95	6.00	6.03	6.05
4	1.10	3.09	4.19	4.38	4.46	4.50	4.52	4.54
5	0.86	2.46	3.35	3.50	3.57	3.60	3.61	3.63
6	0.71	2.04	2.79	2.92	2.97	3.00	3.01	3.02
7	0.60	1.74	2.40	2.50	2.55	2.57	2.58	2.59
8	0.52	1.52	2.10	2.18	2.23	2.25	2.26	2.27
9	0.46	1.34	1.87	1.94	1.98	2.00	2.00	2.02
10	0.42	1.21	1.69	1.75	1.78	1.80	1.80	1.81
11	0.38	1.10	1.53	1.59	1.62	1.63	1.64	1.65
12	0.34	1.00	1.41	1.45	1.48	1.50	1.50	1.51
13	0.32	0.93	1.30	1.34	1.37	1.38	1.38	1.39
14	0.29	0.86	1.21	1.25	1.27	1.28	1.29	1.29
15	0.27	0.80	1.13	1.16	1.19	1.20	1.20	1.21
16	0.26	0.75	1.06	1.09	1.11	1.12	1.12	1.13
17	0.24	0.70	1.00	1.02	1.05	1.06	1.06	1.07
18	0.23	0.67	0.95	0.97	0.99	1.00	1.00	1.01

Table C.1.3 First Eigenvalue

ms/md=10.0

Number of Lumps	Stiffness Ratio (kd/ks)							
	0.6169	2.4674	9.8696	22.206	39.478	61.685	88.820	120.90
1	31.19	32.83	33.17	33.20	33.24	33.24	33.24	33.24
2	17.41	18.84	19.11	19.15	19.17	19.17	19.18	19.18
3	12.01	13.17	13.38	13.41	13.43	13.43	13.44	13.44
4	9.15	10.11	10.28	10.31	10.32	10.33	10.33	10.33
5	7.38	8.20	8.35	8.36	8.38	8.39	8.39	8.39
6	6.19	6.90	7.03	7.05	7.06	7.06	7.06	7.06
7	5.33	5.96	6.07	6.09	6.09	6.10	6.10	6.10
8	4.67	5.24	5.34	5.35	5.36	5.36	5.37	5.37
9	4.16	4.67	4.76	4.78	4.78	4.79	4.79	4.79
10	3.75	4.22	4.30	4.32	4.32	4.32	4.32	4.32
11	3.42	3.85	3.92	3.93	3.94	3.94	3.94	3.94
12	3.14	3.53	3.60	3.61	3.62	3.62	3.62	3.62
13	2.90	3.27	3.33	3.34	3.35	3.35	3.35	3.35
14	2.69	3.04	3.10	3.11	3.11	3.11	3.12	3.12
15	2.52	2.84	2.90	2.91	2.91	2.91	2.91	2.91
16	2.36	2.66	2.72	2.73	2.73	2.73	2.73	2.73
17	2.22	2.51	2.56	2.57	2.57	2.57	2.58	2.57
18	2.10	2.37	2.42	2.43	2.43	2.43	2.43	2.43

Table C.2.1 Second Eigenvalue

ms/md=0.1

Number of Lumps	Stiffness Ratio (kd/ks)							
	0.6169	2.4674	9.8696	22.206	39.478	61.685	88.820	120.90
2	17.99	10.76	7.21	8.50	9.22	9.60	9.81	9.94
3	12.37	7.03	3.50	3.80	4.12	4.30	4.41	4.48
4	9.41	5.19	2.15	2.17	2.32	2.42	2.49	2.53
5	7.58	4.09	1.50	1.41	1.49	1.55	1.60	1.62
6	6.35	3.38	1.12	0.99	1.04	1.08	1.11	1.13
7	5.46	2.87	0.89	0.74	0.76	0.79	0.81	0.83
8	4.79	2.50	0.73	0.57	0.59	0.61	0.62	0.63
9	4.26	2.21	0.61	0.46	0.46	0.48	0.49	0.50
10	3.84	1.98	0.52	0.38	0.38	0.39	0.40	0.41
11	3.50	1.79	0.46	0.32	0.31	0.32	0.33	0.33
12	3.21	1.64	0.41	0.27	0.26	0.27	0.28	0.28
13	2.96	1.51	0.36	0.23	0.22	0.23	0.24	0.24
14	2.75	1.40	0.33	0.20	0.19	0.20	0.20	0.21
15	2.57	1.30	0.30	0.18	0.17	0.17	0.18	0.18
16	2.41	1.22	0.28	0.16	0.15	0.15	0.15	0.16
17	2.27	1.14	0.25	0.14	0.13	0.13	0.14	0.14
18	2.15	1.08	0.24	0.13	0.12	0.12	0.12	0.12

Table C.2.2 Second Eigenvalue

ms/md=1.0

Number of Lumps	Stiffness Ratio (kd/ks)							
	0.6169	2.4674	9.8696	22.206	39.478	61.685	88.820	120.90
2	16.13	6.86	9.07	11.53	12.51	12.96	13.22	13.36
3	11.12	4.36	3.92	5.32	5.96	6.25	6.44	6.53
4	8.46	3.16	2.18	3.06	3.52	3.75	3.86	3.92
5	6.81	2.47	1.39	2.00	2.34	2.50	2.60	2.65
6	5.70	2.02	0.97	1.42	1.69	1.81	1.90	1.93
7	4.89	1.71	0.71	1.06	1.29	1.38	1.46	1.49
8	4.28	1.48	0.55	0.83	1.02	1.10	1.16	1.19
9	3.81	1.30	0.43	0.67	0.83	0.90	0.96	0.97
10	3.43	1.16	0.35	0.55	0.70	0.75	0.80	0.82
11	3.11	1.05	0.29	0.46	0.59	0.64	0.69	0.70
12	2.85	0.96	0.25	0.40	0.51	0.56	0.60	0.61
13	2.63	0.88	0.21	0.34	0.45	0.49	0.53	0.54
14	2.44	0.81	0.18	0.30	0.40	0.43	0.47	0.48
15	2.27	0.76	0.16	0.27	0.36	0.39	0.43	0.43
16	2.13	0.71	0.14	0.24	0.33	0.35	0.39	0.39
17	2.00	0.66	0.13	0.21	0.30	0.32	0.35	0.36
18	1.89	0.62	0.11	0.19	0.27	0.29	0.32	0.33

Table C.2.3 Second Eigenvalue

ms/md=10.0

Number of Lumps	Stiffness Ratio (kd/ks)							
	0.6169	2.4674	9.8696	22.206	39.478	61.685	88.820	120.90
2	2.33	20.06	25.48	26.12	26.32	26.41	26.46	26.48
3	1.37	10.99	15.82	16.39	16.57	16.65	16.69	16.72
4	0.98	7.19	11.25	11.74	11.89	11.96	12.00	12.02
5	0.77	5.23	8.65	9.08	9.21	9.27	9.30	9.32
6	0.63	4.06	7.00	7.37	7.49	7.54	7.57	7.58
7	0.53	3.29	5.87	6.19	6.30	6.34	6.36	6.38
8	0.46	2.76	5.05	5.34	5.43	5.47	5.49	5.50
9	0.40	2.37	4.42	4.68	4.76	4.80	4.82	4.83
10	0.36	2.07	3.93	4.17	4.24	4.28	4.29	4.30
11	0.33	1.83	3.54	3.76	3.82	3.85	3.87	3.88
12	0.30	1.65	3.21	3.42	3.48	3.51	3.52	3.53
13	0.27	1.49	2.94	3.13	3.19	3.22	3.23	3.24
14	0.25	1.36	2.72	2.89	2.95	2.97	2.98	2.99
15	0.24	1.25	2.52	2.69	2.74	2.76	2.77	2.78
16	0.22	1.16	2.35	2 51	2.56	2.58	2.59	2.60
17	0.21	1.08	2.20	2.35	2.40	2.42	2.43	2.43
18	0.20	1.01	2.07	2.21	2.25	2.27	2.28	2.29

Table C.3.1 Third Eigenvalue

ms/md=0.1

Number of Lumps	Stiffness Ratio (kd/ks)							
	0.6169	2.4674	9.8696	22.206	39.478	61.685	88.820	120.90
3	20.82	19.53	13.83	15.01	15.95	16.45	16.74	16.91
4	15.15	13.80	8.65	8.58	9.06	9.37	9.56	9.68
5	11.80	10.54	6.10	5.61	5.84	6.03	6.16	6.24
6	9.63	8.46	4.62	3.99	4.09	4.21	4.29	4.35
7	8.10	7.04	3.66	3.00	3.02	3.10	3.16	3.20
8	6.99	6.01	3.01	2 35	2.33	2.38	2.42	2.45
9	6.13	5.23	2.53	1.90	1.85	1.88	1.91	1.94
10	5.46	4.63	2.18	1.58	1.51	1.53	1.55	1.57
11	4.92	4.15	1.90	1.33	1.26	1.27	1.28	1.29
12	4.48	3.75	1.68	1.14	1.06	1.07	1.08	1.09
13	4.10	3.43	1.51	0.99	0.91	0.91	0.92	0.92
14	3.79	3.15	1.36	0.87	0.79	0.78	0.79	0.80
15	3.52	2.92	1.24	0.78	0.69	0.68	0.69	0.69
16	3.28	2.71	1.14	0.70	0.61	0.60	0.60	0.61
17	3.07	2.54	1.05	0.63	0.55	0.53	0.53	0.54
18	2.89	2.38	0.98	0.57	0.49	0.48	0.48	0.48

Table C.3.2 Third Eigenvalue

ms/md=1.0

Number of Lumps	Stiffness Ratio (kd/ks)							
	0.6169	2.4674	9.8696	22.206	39.478	61.685	88.820	120.90
3	20.82	18.80	13.68	15.93	17.15	17.62	17.99	18.12
4	15.16	13.29	8.04	8.94	9.79	10.12	10.42	10.51
5	11.82	10.14	5.47	5.72	6.32	6.53	6.77	6.82
6	9.65	8.14	4.04	3.98	4.42	4.55	4.76	4.78
7	8.13	6.77	3.14	2.94	3.27	3.35	3.53	3.53
8	7.01	5.78	2.54	2.26	2.53	2.57	2.72	2.71
9	6.16	5.04	2.11	1.79	2.02	2.03	2.17	2.15
10	5.49	4.45	1.79	1.46	1.65	1.64	1.77	1.74
11	4.95	3.99	1.55	1.21	1.38	1.35	1.48	1.44
12	4.51	3.61	1.37	1.02	1.17	1.14	1.25	1.21
13	4.14	3.30	1.21	0.87	1.01	0.97	1.08	1.03
14	3.82	3.03	1.09	0.76	0.88	0.83	0.94	0.89
15	3.55	2.81	0.99	0.66	0.78	0.72	0.82	0.78
16	3.32	2.61	0.90	0.59	0.70	0.63	0.73	0.68
17	3.11	2.44	0.83	0.52	0.63	0.56	0.65	0.60
18	2.93	2.30	0.77	0.47	0.57	0.50	0.59	0.54

Table C.3.3 Third Eigenvalue

ms/md=10.0

Number of Lumps	Stiffness Ratio (kd/ks)							
	0.6169	2.4674	9.8696	22.206	39.478	61.685	88.820	120.90
3	20.12	10.49	23.00	24.91	25.46	25.68	25.80	25.87
4	14.63	5.84	14.41	16.25	16.77	17.00	17.11	17.18
5	11.39	4.10	9.96	11.62	12.10	12.30	12.41	12.47
6	9.28	3.15	7.38	8.85	9.28	9.46	9.55	9.61
7	7.81	2.54	5.74	7.05	7.43	7.59	7.68	7.73
8	6.73	2.12	4.63	5.80	6.15	6.29	6.37	6.42
9	5.91	1.82	3.84	4.90	5.21	5.34	5.42	5.46
10	5.26	1.59	3.25	4.22	4.51	4.63	4.69	4.73
11	4.74	1.41	2.80	3.69	3.96	4.07	4.13	4.16
12	4.31	1.27	2.45	3.27	3.52	3.62	3.68	3.71
13	3.95	1.15	2.17	2.93	3.16	3.26	3.31	3.34
14	3.64	1.06	1.95	2.65	2.87	2.96	3.01	3.03
15	3.38	0.97	1.76	2.42	2.62	2.70	2.75	2.77
16	3.15	0.91	1.60	2.22	2.41	2.49	2.53	2.56
17	2.96	0.85	1.46	2.05	2.23	2.30	2.34	2.37
18	2.78	0.80	1.34	1.90	2.07	2.14	2.18	2.20

Table C.4.1 Fourth Eigenvalue

ms/md=0.1

Number of Lumps	Stiffness Ratio (kd/ks)							
	0.6169	2.4674	9.8696	22.206	39.478	61.685	88.820	120.90
4	22.25	22.49	18.61	19.11	20.05	20.58	20.89	21.08
5	16.80	16.79	13.19	12.48	12.98	13.35	13.58	13.74
6	13.32	13.19	9.97	8.89	9.10	9.34	9.51	9.63
7	10.95	10.75	7.88	6.71	6.75	6.90	7.02	7.11
8	9.25	9.02	6.43	5.28	5.22	5.31	5.39	5.46
9	7.97	7.73	5.38	4.28	4.16	4.21	4.27	4.32
10	6.99	6.74	4.60	3.55	3.39	3.42	3.46	3.50
11	6.21	5.97	3.99	3.01	2.83	2.83	2.87	2.90
12	5.58	5.34	3.51	2.58	2.40	2.39	2.41	2.43
13	5.06	4.82	3.13	2.25	2.06	2.04	2.05	2.07
14	4.63	4.40	2.81	1.98	1.79	1.76	1.77	1.78
15	4.26	4.03	2.55	1.77	1.57	1.54	1.54	1.55
16	3.94	3.72	2.32	1.59	1.39	1.35	1.35	1.36
17	3.67	3.46	2.13	1.43	1.24	1.20	1.20	1.20
18	3.43	3.22	1.97	1.30	1.11	1.07	1.07	1.07

Table C.4.2 Fourth Eigenvalue

ms/md=1.0

Number of Lumps	Stiffness Ratio (kd/ks)							
	0.6169	2.4674	9.8696	22.206	39.478	61.685	88.820	120.90
4	22.34	22.43	18.13	19.48	20.70	21.15	21.57	21.67
5	16.90	16.73	12.63	12.55	13.42	13.74	14.12	14.18
6	13.42	13.14	9.50	8.82	9.41	9.61	9.93	9.95
7	11.06	10.71	7.48	6.57	6.97	7.08	7.36	7.35
8	9.36	8.99	6.10	5.11	5.39	5.43	5.68	5.64
9	8.09	7.70	5.10	4.10	4.30	4.29	4.51	4.46
10	7.10	6.72	4.36	3.37	3.52	3.47	3.68	3.62
11	6.33	5.95	3.79	2.83	2.94	2.87	3.06	2.99
12	5.70	5.32	3.33	2.42	2.50	2.41	2.59	2.51
13	5.18	4.81	2.97	2.09	2.15	2.05	2.22	2.13
14	4.74	4.39	2.67	1.83	1.88	1.76	1.93	1.83
15	4.36	4.03	2.43	1.62	1.66	1.53	1.69	1.59
16	4.06	3.72	2.22	1.44	1.48	1.34	1.50	1.40
17	3.78	3.45	2.04	1.29	1.33	1.19	1.34	1.23
18	3.54	3.22	1.89	1.17	1.20	1.06	1.20	1.09

Table C.4.3 Fourth Eigenvalue

ms/md=10.0

Number of Lumps	Stiffness Ratio (kd/ks)							
	0.6169	2.4674	9.8696	22.206	39.478	61.685	88.820	120.90
4	22.23	19.69	21.69	24.86	25.78	26.15	26.34	26.46
5	16.77	14.84	13.85	16.92	17.84	18.22	18.41	18.52
6	13.30	11.68	9.49	12.26	13.12	13.48	13.66	13.76
7	10.93	9.52	6.88	9.31	10.09	10.43	10.59	10.69
8	9.23	7.97	5.20	7.33	8.05	8.35	8.50	8.60
9	7.95	6.82	4.07	5.94	6.59	6.87	7.01	7.10
10	6.97	5.94	3.26	4.92	5.52	5.78	5.91	5.99
11	6.19	5.24	2.67	4.15	4.70	4.94	5.06	5.14
12	5.56	4.68	2.23	3.56	4.07	4.29	4.40	4.47
13	5.05	4.23	1.83	3.09	3.56	3.77	3.88	3.94
14	4.61	3.84	1.61	2.71	3.15	3.35	3.45	3.51
15	4.24	3.52	1.39	2.41	2.82	3.00	3.09	3.15
16	3.93	3.25	1.21	2.15	2.54	2.71	2.80	2.85
17	3.65	3.01	1.06	21.94	2.30	2.46	2.55	2.60
18	3.41	2.80	0.94	1.75	2.10	2.25	2.33	2.38

Table C.5.1 Fifth Eigenvalue

ms/md=0.1

Number of Lumps	Stiffness Ratio (kd/ks)							
	0.6169	2.4674	9.8696	22.206	39.478	61.685	88.820	120.90
5	23.70	24.11	22.25	21.89	22.75	23.26	23.57	23.76
6	18.47	19.71	16.83	15.56	16.00	16.38	16.63	16.79
7	14.92	15.06	13.25	11.77	11.89	12.14	12.33	12.46
8	12.40	12.47	10.76	9.27	9.20	9.36	9.50	9.60
9	10.54	10.56	8.95	7.53	7.35	7.43	7.54	7.61
10	9.11	9.10	7.60	6.26	6.01	6.05	6.12	6.18
11	8.00	7.97	6.56	5.31	5.02	5.02	5.07	5.11
12	7.11	7.06	5.74	4.57	4.26	4.23	4.27	4.30
13	6.38	6.32	5.08	3.98	3.66	3.62	3.64	3.66
14	5.78	5.71	4.54	3.51	3.18	3.13	3.14	3.16
15	5.27	5.20	4.09	3.13	2.80	2.73	2.73	2.75
16	4.84	4.76	3.71	2.81	2.48	2.41	2.40	2.41
17	4.47	4.39	3.39	2.54	2.21	2.14	2.13	2.14
18	4.15	4.07	3.11	2.31	1.99	1.91	1.90	1.90

Table C.5.2 Fifth Eigenvalue

ms/md=1.0

Number of Lumps	Stiffness Ratio (kd/ks)							
	0.6169	2.4674	9.8696	22.206	39.478	61.685	88.820	120.90
5	23.85	24.11	21.93	22.06	23.23	23.59	24.08	24.11
6	18.63	18.71	16.63	15.53	16.38	16.61	17.09	17.07
7	15.09	15.05	13.14	11.64	12.18	12.30	12.73	12.67
8	12.58	12.46	10.72	9.11	9.45	9.46	9.85	9.76
9	10.72	10.55	8.96	7.36	7.56	7.50	7.85	7.74
10	9.30	9.10	7.65	6.09	6.20	6.08	6.41	6.28
11	8.18	6.96	6.63	5.14	5.20	5.03	5.34	5.19
12	7.29	7.06	5.83	4.40	4.43	4.23	4.52	4.36
13	6.56	6.32	5.19	3.83	3.83	3.61	3.89	3.71
14	5.96	5.71	4.66	3.36	3.35	3.11	3.38	3.20
15	5.46	5.20	4.23	2.98	2.96	2.71	2.97	2.78
16	5.03	4.76	3.86	2.67	2.65	2.38	2.63	2.44
17	4.66	4.39	3.55	2.41	2.38	2.11	2.35	2.15
18	4.34	4.07	3.28	2.19	2.16	1.88	2.12	1.91

Table C.5.3 Fifth Eigenvalue

ms/md=10.0

Number of Lumps	Stiffness Ratio (kd/ks)							
	0.6169	2.4674	9.8696	22.206	39.478	61.685	88.820	120.90
5	23.70	23.85	21.93	25.17	26.36	26.86	27.11	27.26
6	18.47	18.46	14.95	17.89	19.10	19.61	19.86	20.01
7	14.92	14.83	10.89	13.29	14.43	14.92	15.17	15.31
8	12.40	12.26	8.37	10.23	11.28	11.74	11.98	12.11
9	10.53	10.37	6.68	8.10	9.06	9.49	9.71	9.83
10	9.11	8.94	5.49	6.56	7.44	7.83	8.04	8.16
11	8.00	7.81	4.61	5.42	6.22	6.59	6.78	6.89
12	7.10	6.92	3.95	4.55	5.28	5.62	5.80	5.90
13	6.37	6.19	3.43	3.87	4.55	4.86	5.03	5.12
14	5.77	5.59	3.01	3.33	3.95	4.25	4.40	4.49
15	5.26	5.08	2.67	2.89	3.47	3.76	3.90	3.98
16	4.83	4.66	2.39	2.53	3.07	3.33	3.47	3.55
17	4.46	4.29	2.16	2.24	2.74	2.99	3.12	3.19
18	4.14	3.98	1.96	1.99	2.46	2.69	2.82	2.89

BIBLIOGRAPHY

BIBLIOGRAPHY

1. Timoshenko, S., Young, D.H., and Weaver, W., Vibration Problems in Engineering, John Wiley and Sons, Inc., 1974.

2. Skelton, R.E., "Observability Measures and Performance Sensitivity in the Model Reduction Problem", Int. J. Control, 29(1979), pp541-556.

3. Aoki, M., "Control of Large-Scale Dynamic Systems by Aggregation", IEEE Trans-AC, 13(1968), pp173-182.

4. Aoki, M., "Some Approximation Methods for Estimation and Control of Large Scale Systems", IEEE Trans-AC, 23(1978), pp173-182.

5. Davison, E.J., "A Method for Simplifying Linear Dynamic Systems", IEEE Trans-AC, 11(1966), pp93-101.

6. Davison, E.J., "A New Method for Simplifying Large Linear Dynamic Systems", IEEE Trans-AC (Correspondence), 13(1968),pp214-215.

7. Jacquot, R.G., and Soedel, W., "Vibrations of Elastic Surface Systems Carrying Dynamic Elements", J. Acoust. Soc. Am., 47(1970),pp1354-1358.

8. Young, D., "Vibration of a Beam with Concentrated Mass, Spring, and Dashpot", Trans ASME, J. Appl. Mech., 70(1948), pp65-72.

9. Crawford, C.R., "A Stable Generalized Eigenvalue Problem", SIAM J. Numer. Anal., 6(1976), pp854-860.

10. Rosenberg, R.C., "A Users Guide to ENPORT-5", The Case Center for Computer Aided Design, Michigan State University, East Lansing, MI., 1983.

11. Dix, R.C., "A Users Manual for MEDUSA (MEchanism-Dynamics -Universal-System-Analyzer)", Mechanics, Mechanical and Aerospace Engineering Department, Illinois Institute of Technology, Chicago, Ill., Jan., 1975.

12. Goudreau, G.L., "Evaluation of Discrete Methods for the Linear Dynamic Response of Elastic and Viscoelastic Solids", SESM Rpt 69-15, University of California at Berkeley (1970).

General References

13. Rayleigh, J.W.S., The Theory of Sound, Vol. I, Dover Publications, Inc., 1945.

14. Hildebrand, F.B., Finite Difference Equations and Simulations, Prentice-Hall, Inc., 1968.

15. Parlett, B.N., The Symmetric Eigenvalue Problem, Prentice-Hall, Inc., 1980.

16. Wilkinson, J.H., The Algebraic Eigenvalue Problem, Oxford University Press, 1965.

17. Sandell, N.R., Varaiya, P., Athans, M., and Safonov, M.G., "Survey of Decentralized Control Methods for Large Scale Systems", IEEE Trans-AC, 23(1978), pp108-128.

18. Kwatny, H.G., and Mablekos, V.E., "The Modelling of Dynamical Processes", IEEE Decision and Control Conference, Houston, 1975.

19. Milne, R.D., "The Analysis of Weakly Coupled Dynamical Systems", Int. J. Control, 2(1965), pp171-199.

20. Dowell, E.H., "On Some General Properties of Combined Dynamical Systems", Trans ASME, J. Appl. Mech., 40(1970), pp206-209.

21. Belytschko, T., and Mindle, W.L., "Flexural Wave Propagation Behavior of Lumped Mass Approximations", Comp. and Struc., 12(1980), pp805-812.

22. Crede, C.E., and Harris, C.M., Shock and Vibration Handbook, Vol. I, McGraw-Hill, 1961.